Proc. R. Soc. Lond. A **418**, 165–197 (1988)
Printed in Great Britain

Spin reversal of the rattleback: theory and experiment

By A. Garcia and M. Hubbard
Department of Mechanical Engineering, University of California, Davis, California 95616, *U.S.A.*

(*Communicated by Sir Hermann Bondi, F.R.S. – Received* 4 *September* 1987 – *Revised* 10 *February* 1988)

The behaviour of a top known variously as the rattleback, celt or wobblestone is studied. When spun on a flat, smooth, horizontal surface, self-induced oscillations about a horizontal axis eventually consume the initial spin energy; once the spinning has ceased, the oscillations decay and the body spins in the opposite direction. Many rattlebacks seem to be spin biased, reversing spin direction only once and only if the initial spin has the proper sense; others reverse readily from either initial spin direction. Analysis and simulation papers appearing over the past century have attempted, respectively, to explain and qualitatively predict the top's possible behaviours, and to reconcile observed behaviour with various numerical models. In this work, the two broad theories proposed to explain the spin bias, one which neglects slipping and dissipation and one which incorporates these effects, are critically investigated by several means. The validity of the no-slip assumption is questioned. A numerical model which allows for aerodynamic effects and dry friction due to spinning and slipping is developed. The complicated equations of the numerical model are simplified by analysing the transfer of energy between the spin and oscillations. A comprehensive explanation of the behaviour based on this simplified spin model and the realistic limits of the no-slip motion is proposed. Finally, the predictions of the 'complete' numerical model and the simplified model are compared with experimental data.

1. Introduction

The rattleback (also called a celt or wobblestone), a rigid mechanical top with a smoothly curved oblong lower surface, displays some very curious dynamic behaviour when spun on a smooth horizontal surface. Many appear to be biased for spin in one direction, so much so that they will reverse spin direction when spun in the opposite direction. Others exhibit several reversals before eventually coming to rest. Previous analyses of the linearized no-slip dissipation-free equations of motion have demonstrated how an inertial asymmetry makes spin reversals possible. It is not in dispute, here, that the main observed behaviours, single and multiple reversals, can be exhibited by such a model or that the reversal mechanism depends critically on the inertial asymmetry. As is shown presently, however, in many cases unreasonably large values of the friction coefficient are required to account for single reversals with a no-slip dissipation-free model. Such a model also predicts that any rattleback can reverse in both directions with the proper initial conditions, contrary to what one often observes.

If a no-slip dissipation-free model cannot adequately explain commonly observed behaviour, then it is important to understand the essential aspects of the simplest dynamic model which can. Some of our recent physical experiments and computer studies will support the development of such a model, which will comprise the main portion of this paper. To motivate the work below and to place previous efforts in historical context, we first present a brief literature review.

The original paper on the rattleback was written by G. T. Walker (1896) and the analysis therein has proved remarkably durable. Assuming an elliptic paraboloid shape and dissipation-free rolling without slip, he showed that the structure of the dynamic equations changes dramatically when inertial asymmetry exists. Thus he demonstrated the crucial role which the non-coincidence of the horizontal principal axes of inertia and the directions of maximum and minimum curvature at the equilibrium contact point must play in any explanation of the rattlebck phenomenon. By studying the linearized fourth-order characteristic equation, Walker showed that purely stable pitching and rolling oscillations could occur only in one spin direction and then only with a large enough spin magnitude. Interestingly though, Walker did not believe that the stable oscillations were a necessary aspect of the spin bias which he asserted, without a precise investigation, was a property that rattlebacks with very slight inertial asymmetry could exhibit. He also investigated the initial development of the spin from purely oscillatory initial conditions. This paper was somewhat terse and difficult to read, which may account for an apparent lack of awareness by some later authors of the extent of its conclusions.

Because the spin differential equation contains no linear terms, it is not possible to discuss the evolution of the spin directly using a linearized model. Recently, however, Bondi (1986), using the same starting points as Walker (1896), clarified and extended Walker's results by using root locus and conservation of energy arguments to understand indirectly how the spin evolves. He showed clearly that several types of rattlebacks exist, categorized by the different spin dependent stability of the pitching and rolling oscillations they exhibit, and thus explained how the possibility of reversals in one or both directions depends solely on the geometric and inertial parameters of the body. Bondi again demonstrated that when stable oscillations and spin can exist, the magnitude of the spin angular velocity must be greater than a critical value, n_{c1}. Bondi, however, in his description of the spin evolution of a body which reverses and then spins stably, neglected to examine the magnitude of the friction forces required for such a motion to be possible and the conditions under which the no-slip assumption was reasonable.

The no-slip assumption was questioned in the two papers by Magnus (1971, 1974) in which a quasi-viscous (linear) relation between the friction force and the velocity of the contact point was assumed (continuous slipping). The order of the characteristic equation for the linearized motion increased to six and its coefficients became so complicated that no general conclusions about stability were possible. Magnus (1974) was able to demonstrate, however, that cases exist where stability depends only on the sign of spin, and therefore that the inclusion of viscous slip changed the requirement of Walker and Bondi that stable oscillations are only possible at spin rates above n_{c1}. Both of these papers motivate the development of a realistic model which predicts if and when slip occurs and, more generally, the effect of slipping on the dynamic behaviour.

Caughey (1980), using a model of questionable physical validity, applied an asymptotic perturbation approach to show that Euler's equations with small viscous damping in all three axes and linear springs about the horizontal ones could 'capture the essential features of the rattleback'. He concluded that in the absence of any dissipation reversals occur in both spin directions and that dissipation could cause the observed spin bias. Lindberg & Junkins (1984), in a search for the 'essential geometric and mass properties which delineate the two (completely unstable and stable in only one direction) types', proposed a nonlinear perturbation analysis approach to answer the 'remaining' question, 'Under the assumption of a conservative system (no dissipative friction) can the system ever possess a stable spin equilibrium?' Even though they referenced the paper of Walker (1896), they failed to recognize that this was precisely the question that Walker had answered.

The spate of studies in the 1980s seems to have been spurred, at least partly, by a popular article by J. Walker (1979) which qualitatively described the behaviour and pictured specimens which reversed in one or both directions. Two of these more recent studies, Lindberg & Longman (1983) and Kane & Levinson (1982), which appeared nearly simultaneously and relied principally on numerical solutions of the exact nonlinear equations of motion, contained similar conclusions albeit based on somewhat different models. Lindberg & Longman (1983) simulated exactly the model proposed by Walker (1896) and the simulations showed that Walker's full model can predict reversals. They found that the times for reversals to take place may differ substantially for the different spin directions (15 s, 250 s). A preoccupation with integration over these long times (one 400 s simulation was presented!) seems to have drawn Lindberg & Longman (1983) away from a realistic investigation of important dissipative mechanisms. An interesting result was the proof that, due to gyroscopic terms in the linearized equations, there is no technique that will decouple the system in second-order form to yield two independent oscillatory modes.

Kane & Levinson (1982), in the only paper to assume an ellipsoidal shape, again raised the important issue of the role of dissipation in explanations of the spin bias. They demonstrated that the addition of a viscous retarding torque about all three axes could suppress reversals observed in simulations where the dissipation was neglected. The results showed that the phenomenon of reversal is not sensitive to second-order surface shape effects and suggested that an explanation of the spin bias exhibited by many real rattlebacks requires an allowance for some dissipative mechanism.

The survey of the available literature indicates that two conflicting explanations of the spin bias have been proposed. One theory, espoused most convincingly by Bondi (1986), neglects slipping and dissipation and asserts that these factors are unimportant; the curious behaviour is a property of a particular class of bodies characterized solely by their inertial and geometric qualities. According to the other, slipping and/or dissipation play an important role in suppressing reversal in one spin direction.

The literature also reveals the shortcomings of the principal methods used in trying to understand the rattleback's behaviour, stability analysis of the linearized equations of motion and numerical solutions of the complete nonlinear equations. Specifically, any linearizable equations of motion must be derived under restrictive or even unrealistic assumptions, i.e. no slipping or other dissipation (Walker 1896; Bondi 1986), viscous friction (Magnus 1971, pp. 19–23; 1974). Also, because of the nature of the spin differential equation, linearized equations cannot predict the spin evolution directly. On the other hand, particular numerical solutions do not provide a comprehensive picture of the behaviour. Indeed, those who have relied on simulation have failed to discover or investigate the variety of behaviours, predicted by Bondi (1986), which a no-slip dissipation-free model may exhibit.

In §2, the characteristic time domain behaviour of the different types of rattlebacks delineated by Bondi is investigated by simulation; it is thus verified that Walker's (1896) original model can exhibit the qualitatively different spin behaviours which are commonly observed. However, as is shown in §3, in many cases unrealistically large values of the friction coefficient are required to explain single reversals using Walker's model. A numerical model incorporating several dissipative effects including slipping is proposed in §4 which can exhibit single reversals with realistic values of the friction coefficient. The complexity of the underlying equations, however, make the numerical model inappropriate as a source of understanding of the phenomenon. Toward that end, a simple dynamic model of the spin behaviour is developed in §5 which adequately explains the apparent spin bias many real rattlebacks exhibit. Finally the predictions of the complete model and the simple spin dynamic model are compared with accurate experimental data in §6.

2. The energy conservative case

(a) *Development of the equations of motion*

We begin by developing the simplest useful set of dynamic equations, those studied by G. T. Walker (1896), Lindberg & Longman (1983), Lindberg & Junkins (1984) and Bondi (1986), in which dissipation is neglected and the body is assumed to roll without slipping on a flat horizontal surface. Straightforward application of Newton's law provides the simplest derivation and most compact expression of the governing dynamic equations. Dotted quantities represent derivatives in the body-fixed frame in which all the vectors are coordinatized. The notation of Bondi (1986) is used where possible; it is given here.

g_c, gravitational constant
M, mass of the body
I, diagonal inertia matrix (with elements I_{11}, I_{22}, I_{33} about the 1, 2, and 3 axes, respectively)
f, contact force

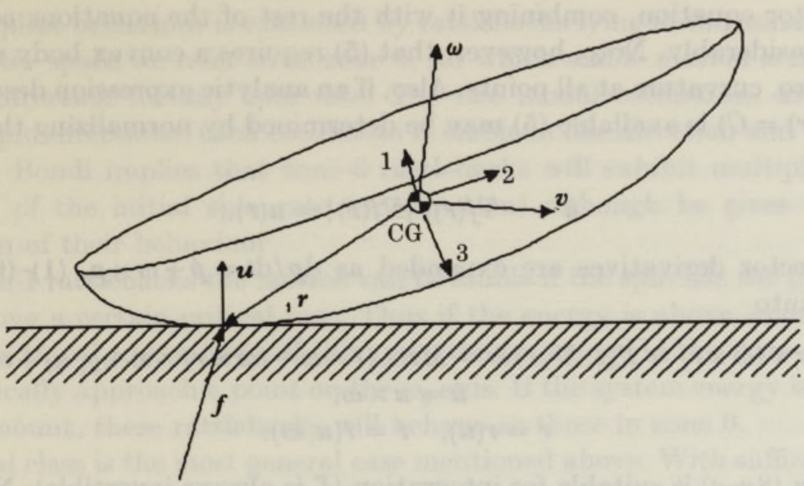

FIGURE 1. Notation: $\boldsymbol{f}$, contact force; $\boldsymbol{r}$, contact point position relative to CG; $\boldsymbol{u}$, unit normal to body surface at the contact point; $\boldsymbol{v}$, velocity of CG; 123, body fixed principal axes.

$\boldsymbol{v}$, velocity of the body CG
$\boldsymbol{\omega}$, angular velocity of body
$\boldsymbol{h}$, angular momentum of body
$\boldsymbol{r}$, contact point in body fixed principal axes
$\boldsymbol{u}$, unit vector normal to the body's surface at the point of contact
a, equilibrium distance from CG to contact point
n, spin, $n = \boldsymbol{u} \cdot \boldsymbol{\omega}$
ξ, angle about the 3-axis between the direction of least curvature and the 1-axis (skew angle)

Summing forces and moments, we have

$$M\,\mathrm{d}\boldsymbol{v}/\mathrm{d}t = \boldsymbol{f} - Mg_c\,\boldsymbol{u}, \tag{1}$$

$$\mathrm{d}\boldsymbol{h}/\mathrm{d}t = \boldsymbol{r} \times \boldsymbol{f}, \tag{2}$$

and because $\boldsymbol{u}$ is invariant in inertial space

$$\dot{\boldsymbol{u}} = \boldsymbol{u} \times \boldsymbol{\omega}, \tag{3}$$

where $\boldsymbol{\omega}$ is related to $\boldsymbol{h}$ by

$$\boldsymbol{h} = \boldsymbol{I}\boldsymbol{\omega}. \tag{4}$$

We have four equations ((1)–(4)) in the six dynamic vectors: $\boldsymbol{f}$, $\boldsymbol{v}$, $\boldsymbol{\omega}$, $\boldsymbol{h}$, $\boldsymbol{r}$, $\boldsymbol{u}$. It remains to make appropriate assumptions to fix the extra degrees of freedom. The assumptions made for the energy conservative equations are: the body remains in contact with the flat, horizontal surface upon which it spins and the point of contact has zero velocity. The former implies that

$$\boldsymbol{r} = \boldsymbol{r}(\boldsymbol{u}), \tag{5}$$

and the latter that

$$\boldsymbol{v} = \boldsymbol{r} \times \boldsymbol{\omega}. \tag{6}$$

We delay in writing the exact form of (5) because it depends on the specific shape of the body and we would like to develop a general set of dynamic equations. Another reason for delaying is that, because (5) is generally not expressible as a simple vector equation, combining it with the rest of the equations complicates matters considerably. Note, however, that (5) requires a convex body with finite, but non-zero, curvature at all points. Also, if an analytic expression describing the surface ($f(\boldsymbol{r}) = C$) is available (5) may be determined by normalizing the gradient vector:

$$\boldsymbol{u} = -\nabla f(\boldsymbol{r})/|\nabla f(\boldsymbol{r})| = \boldsymbol{u}(\boldsymbol{r}). \tag{7}$$

If the vector derivatives are expanded as $\mathrm{d}\boldsymbol{p}/\mathrm{d}t = \dot{\boldsymbol{p}} + \boldsymbol{\omega} \times \boldsymbol{p}$, (1)–(6) may be combined into

$$\begin{gathered} \boldsymbol{I}\dot{\boldsymbol{\omega}} + M\boldsymbol{r} \times (\dot{\boldsymbol{\omega}} \times \boldsymbol{r}) = \boldsymbol{I}'(\boldsymbol{I}, M, \boldsymbol{r})\,\dot{\boldsymbol{\omega}} = M\boldsymbol{r} \times (\dot{\boldsymbol{r}} \times \boldsymbol{\omega} + (\boldsymbol{\omega} \times \boldsymbol{r}) \times \boldsymbol{\omega} + g_{\mathrm{c}}\boldsymbol{u}) - \boldsymbol{\omega} \times (\boldsymbol{I}\boldsymbol{\omega}), \\ \dot{\boldsymbol{u}} = \boldsymbol{u} \times \boldsymbol{\omega}, \\ \boldsymbol{r} = \boldsymbol{r}(\boldsymbol{u}), \quad \dot{\boldsymbol{r}} = \dot{\boldsymbol{r}}(\boldsymbol{u}, \boldsymbol{\omega}). \end{gathered} \tag{8a–c}$$

Equation (8a–c) is suitable for integration ($\boldsymbol{I}'$ is always invertible). Note that $\boldsymbol{r}$ and $\dot{\boldsymbol{r}}$ are algebraically determined by $\boldsymbol{\omega}$ and $\boldsymbol{u}$. The components of $\boldsymbol{u}$ are not all independent because $\boldsymbol{u}$ has unit length. Thus there are only five state variables, the three components of $\boldsymbol{\omega}$ and two components of $\boldsymbol{u}$. Also, the particular geometry is not specified.

(b) *Analysis of the linearized dissipation-free equations*

Major portions of the analyses of Walker (1896) and Bondi (1986) were devoted to studying the above equations linearized about the line in the state space coinciding with the ω_3-axis. Because the coupled differential equation describing the evolution of ω_3 involves only terms of the second order and above, this amounts to making the spin a quasi-constant (this type of analysis is not possible if linear torsional damping is included). Hence the dynamics remaining in the fourth-order characteristic equation are those of the pitching and rolling of the body at some nominal spin. The stability of these oscillations may be studied directly, and the evolution of the spin indirectly by realizing that energy must be conserved among the three storage mechanisms; spin and the two independent oscillations.

Both Walker (1896) and Bondi (1986) developed (5) by assuming that one principal axis of inertia (the 3-axis) coincided with the intersection of the symmetry planes of the elliptic paraboloid lower surface; the asymmetry of the body was due to the horizontal principal axes lying outside of the symmetry planes. A more general asymmetry in which the 3-axis did not coincide with the inertial vertical at equilibrium would complicate the analysis severely because the derivation of non-zero spin equilibria would no longer be such a trivial matter. The complete nonlinear equations for arbitrarily oriented principal inertia axes, however, may be developed in a straightforward manner from (8).

In the most general case (see below), both Walker (1896) and Bondi (1986) concluded that completely stable motion is possible in only one spin direction, and only if the magnitude of the spin lies between an upper and lower bound. What emerges much more clearly from Bondi's analysis is the existence of three regions in the inertial and geometric parameter space, each characterized by different spin-dependent behaviour.

The simplest behaviour is exhibited by rattlebacks lying in the unnamed region of parameter space we refer to as zone 0, for which stable motion is not possible in either direction for any spin rate. The two modal oscillations are stable in opposite spin directions; each oscillation is stable in one direction and unstable in the other. Bondi implies that zone-0 rattlebacks will exhibit multiple reversals regardless of the initial spin rate (or direction) although he gives no explicit description of their behaviour.

For zone-I rattlebacks the motion can be stable if the spin has the proper sense and is above a certain critical rate. Thus if the energy is above some minimum ($E > E_{c1} = \frac{1}{2}I_{33}\,n_{c1}^2$) for a body of this type, the trajectory in the state-space must asymptotically approach a point on the ω_3 axis. If the system energy is below this critical amount, these rattlebacks will behave as those in zone 0.

The final class is the most general case mentioned above. With sufficient energy ($E > E_{c2} = \frac{1}{2}I_{33}\,n_{c2}^2$), a zone-II rattleback will attain a high enough spin rate (n_{c2}) so that one pair of the once complex oscillatory roots becomes purely real with one root (or both in some degenerate cases) migrating into the right half-plane. Bondi does not conjecture what the motion of such a rattleback would be. With less energy, this type of rattleback can exhibit the same kinds of behaviour as those in zones 0 and I: if the initial energy is bounded by the two limits ($E_{c1} < E < E_{c2}$), the body tends towards completely stable motion; if it is below the lower limit ($E < E_{c1}$), an infinite number of reversals occur. These regions were defined by Bondi (1986) as follows.

Define α, β and γ by (we assume, without loss of generality that $\alpha > \beta$)

$$I_{11}+Ma^2 = \alpha Ma^2, \quad I_{22}+Ma^2 = \beta Ma^2, \quad I_{33} = \gamma Ma^2 \tag{9}$$

and θ, ϕ, and ψ by

θ, ratio of 'a' to the smaller principal radii of curvature ($\theta < 1$);
ϕ, ratio of 'a' to the larger principal radii of curvature ($\phi < \theta < 1$);
$\psi = \cos^2\xi - \sin^2\xi$.

Then, following Bondi (1986), define μ, κ, λ and ν by

$$\alpha\beta\theta\phi\mu = 2-(\theta+\phi)-(\alpha+\beta-\gamma)(\theta+\phi-2\theta\phi), \tag{10}$$

$$\alpha\beta\theta\phi\kappa = 1-\tfrac{1}{2}(\alpha+\beta-2\gamma)(\theta+\phi)+(\alpha-\gamma)(\beta-\gamma)\theta\phi-\tfrac{1}{2}(\alpha-\beta)(\theta-\phi)\psi, \tag{11}$$

$$\alpha\beta\theta\phi\lambda = \tfrac{1}{2}(\alpha+\beta)(\theta+\phi-2\theta\phi)-\tfrac{1}{2}(\alpha-\beta)(\theta-\phi)\psi, \tag{12}$$

$$\alpha\beta\theta\phi\nu = (1-\theta)(1-\phi). \tag{13}$$

Bondi (1986) showed that $\mu < \kappa$ for all sets of parameters $(\alpha,\beta,\gamma,\theta,\phi,\psi)$. Thus, zone 0 is the region in the six-dimensional parameter space where $\mu > 0$, zone I where $\mu < 0$ and $\kappa > 0$, and zone II where $\kappa < 0$. Because μ is independent of ψ, so is the boundary between zones 0 and I ($\mu = 0$). The critical spins, n_{c1} and n_{c2}, are defined as

$$n_{c1} = \{-(g_c/a)(\nu/\mu)\}^{\frac{1}{2}}, \tag{14}$$

$$n_{c2} = \{2g_c\,\nu/a\}^{\frac{1}{2}}\{[(\lambda+\mu)^2-4\nu\kappa]^{\frac{1}{2}}-(\lambda+\mu)\}^{-\frac{1}{2}}. \tag{15}$$

The most interesting results of the linear analysis are the possibility of completely stable motion without allowance for dissipation, and the discovery by Bondi of the possibility of behaviour, in the zone-II case, unmentioned in the literature. Published simulations which ignored dissipation (Kane & Levinson (1982) studied a zone-0 rattleback; Lindberg & Longman (1983) simulated a zone-I rattleback spinning at below the critical speed) have shown only behaviour of the first type described, multiple reversals, *ad infinitum*. Also, the strange zone-II behaviour associated with real roots of the characteristic equation is difficult to understand without simulation. The first applications for the numerical model are verification of the single reversal phenomenon and further investigation of the time-domain behaviour of the last type (for a zone-II body spinning above both critical speeds). In all subsequent simulations, the shape used to develop (5) is an elliptic paraboloid.

(c) *Simulations of zone-I and zone-II behaviour*

In the first simulations we will investigate the motion of a zone-I body which initially spins in the *unsteady* direction, the direction in which stable motion is not possible at any spin rate. (For zone-0 and zone-II rattlebacks the definition of the *unsteady* spin direction is extended to be the spin direction in which the higher-frequency oscillation is unstable.) The fundamental dimensionless parameters describing this rattleback are: $\theta = 0.9633$, $\phi = 0.0846$, $\psi = 0.8480$, $\alpha = 7.037$, $\beta = 1.644$, $\gamma = 6.431$. One additional parameter, $a = 2.267$ cm is required because dimensional time is used in the simulation. From these we find $\mu = -1.102$, $\kappa = 1.003$ and $n_{c1} = 3.738$ rad/s confirming that the body lies in zone I. Depending on the initial conditions, two different types of behaviour may be expected: if the initial energy is greater than E_{c1} ($= \frac{1}{2} I_{33} n_{c1}^2$), after a single reversal the oscillations should decay resulting in stable spin in the opposite (*steady*) direction. With less energy, the oscillations cannot be stable so that after the first reversal, with enough time, another reversal should occur. The initial conditions for the first simulation in which the system possesses enough energy so that asymptotically stable spin may be achieved are $\boldsymbol{\omega} = [0.0\ 0.0\ -6.0]^t$ rad s^{-1}, $\boldsymbol{u} = [-0.01\ -0.01\ -0.9999]^t$. The spin time history (figure 2) shows a single reversal. To verify that the oscillations after reversal are stable we must examine the orientation of the body. An indicator used by Kane & Levinson (1982) to observe the 'wobble' behaviour was the angle between the inertial vertical and the body's 3-axis. The wobble angle history (figure 2) indicates that the oscillations about the steady spin are decaying and thus stable.

To investigate the change in behaviour when the energy is less than the critical amount we simulate with the same parameters and the initial conditions $\boldsymbol{\omega} = [0.0\ 0.0\ -0.5]^t$ rad s^{-1}, $\boldsymbol{u} = [-0.03\ -0.03\ -0.9991]^t$. The results (figure 3) indicate that after the first reversal, the wobble angle begins to grow very slowly. Also, note that with less initial energy, the maximum value of the wobble angle during reversal is much smaller.

For the zone-II body, we take: $\theta = 0.9633$, $\phi = 0.0846$, $\psi = 0.8660$, $\alpha = 8.983$, $\beta = 1.644$, $\gamma = 6.431$ and $a = 2.267$ cm, and calculate $\mu = -2.295$, $\kappa = -1.344$, and $n_{c2} = 3.992$ rad s^{-1} verifying that the body is of the desired type. In the first

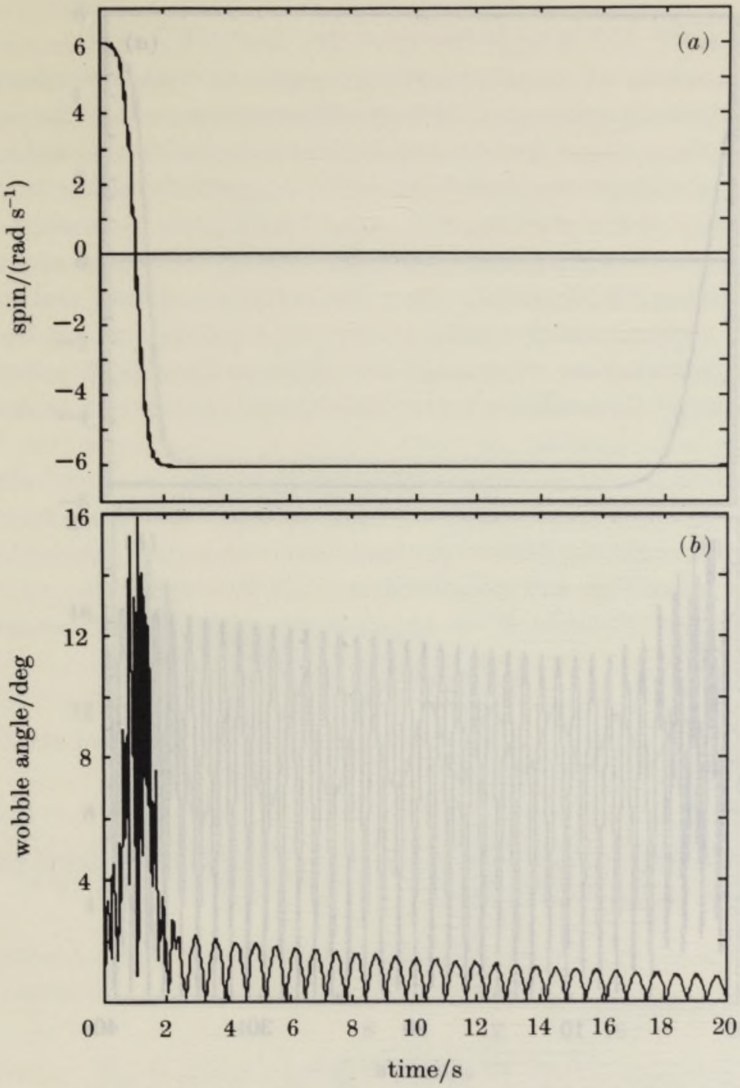

FIGURE 2. Simulated motion of a zone-I rattleback spun initially in unsteady direction, $E > E_{c1}$.

simulation (figure 4) with initial conditions $\boldsymbol{\omega} = [0.0\ 0.0\ -5.0]^t$ rad s^{-1} and $\boldsymbol{u} = [-0.01\ -0.01\ -0.9999]^t$, there is sufficient energy so that characteristic zone-II behaviour is observed. The spin history does not indicate behaviour substantially different than in the above zone-I examples, but the wobble history is very different indeed. The real unstable root signals a change in the character of the equilibrium point. Previously, the unstable imaginary roots were associated with unstable oscillations in which the contact point oscillated about the rest equilibrium contact point. In the zone-II case, it appears, the steady state point of contact is other than the rest equilibrium contact point, and eventually the body tends toward stable spin about an axis other than the body's 3-axis. This was verified for the specific body considered here by running the simulation longer. Simulations in which the total mechanical energy is between the two critical

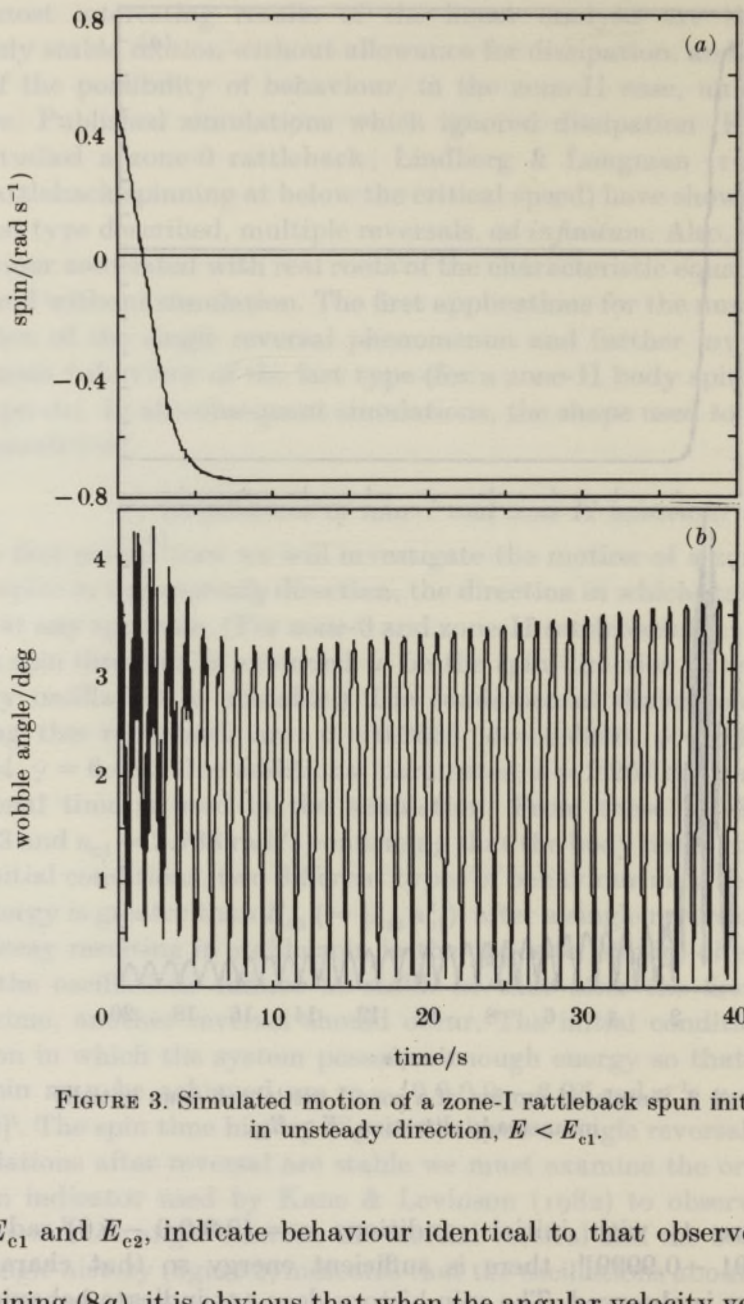

FIGURE 3. Simulated motion of a zone-I rattleback spun initially in unsteady direction, $E < E_{c1}$.

limits, E_{c1} and E_{c2}, indicate behaviour identical to that observed in the zone-I case.

Examining (8*a*), it is obvious that when the angular velocity vector, $\boldsymbol{\omega}$, and the contact point vector, $\boldsymbol{r}$, are vertical, the body is in equilibrium so long as the contact point lies along the body's 3-axis. In this case the angular momentum vector, $\boldsymbol{h}\ (= \boldsymbol{I\omega})$, $\boldsymbol{\omega}$, $\boldsymbol{r}$, and $\boldsymbol{u}$ are all parallel. Further examination reveals that even if $\boldsymbol{r}$ is not vertical, equilibria are possible if the angular momentum vector lies in the vertical plane perpendicular to $\boldsymbol{r} \times \boldsymbol{u}$ and the angular velocity vector remains vertical and has the proper magnitude. In this case the non-zero gravitational and friction torques about the body's CG cause the precession of the angular momentum vector. It can be shown that a sufficient condition for such 'non-trivial' equilibria to exist with $\boldsymbol{r}$ in the neighbourhood of its rest value ($[0\ 0\ a]^t$) is the same as that condition which characterizes a zone-II body, $\kappa < 0$.

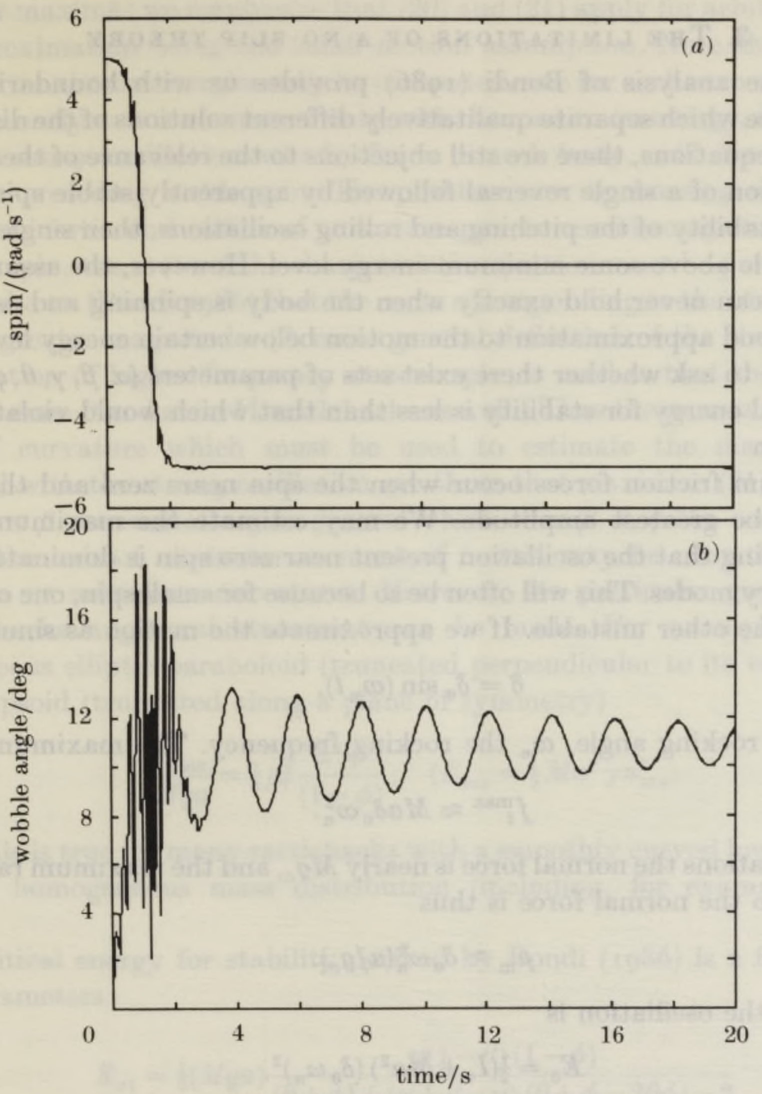

FIGURE 4. Simulated motion of a zone-II rattleback spun initially in unsteady direction, $E > E_{c2}$.

The asymptotic state, then, of a zone-II body when its energy is slightly greater than E_{c2} is spin in the steady direction about an axis perturbed from the 3-axis and a contact point perturbed from the rest equilibrium point. The simulation (figure 4) demonstrates that even if the energy is substantially greater than E_{c1}, an axis of stable spin and an associated contact point can exist. Apparently, there are loci of such stable spin axes and contact points parametrized by the total mechanical energy. The contact point locus breaks away from the rest contact point at the critical energy, E_{c2}. The analytical computation of this locus is complicated by the nature of (5). Although this aspect of the no-slip dissipation-free motion of a rigid body on a plane surface is interesting, it is really a subject separate from the rattleback phenomenon.

3. The limitations of a no-slip theory

Although the analysis of Bondi (1986) provides us with boundaries in the parameter space which separate qualitatively different solutions of the dissipation-free nonlinear equations, there are still objections to the relevance of these results. If an explanation of a single reversal followed by apparently stable spin requires the complete stability of the pitching and rolling oscillations, then single reversals are only possible above some minimum energy level. However, the assumption of no-slip (which can never hold exactly when the body is spinning and oscillating) only yields a good approximation to the motion below certain energy levels. Thus it is reasonable to ask whether there exist sets of parameters $(\alpha, \beta, \gamma, \theta, \phi, \psi)$ such that the critical energy for stability is less than that which would violate the no-slip assumption.

The maximum friction forces occur when the spin nears zero and the body is rocking with the greatest amplitude. We may estimate the maximum friction force by assuming that the oscillation present near zero spin is dominated by one of the oscillatory modes. This will often be so because for small spin, one oscillation is stable and the other unstable. If we approximate the motion as sinusoidal,

$$\delta = \delta_0 \sin(\omega_n t), \tag{16}$$

where δ is the rocking angle, ω_n the rocking frequency. The maximum friction force is about

$$f_t^{\max} \approx Ma\delta_0 \omega_n^2. \tag{17}$$

For small oscillations the normal force is nearly Mg_c, and the maximum ratio of the friction force to the normal force is thus

$$\mu_m \approx \delta_0 \omega_n^2 (a/g_c). \tag{18}$$

The energy in the oscillation is

$$E_0 = \tfrac{1}{2}(I_0 + Ma^2)(\delta_0 \omega_n)^2, \tag{19}$$

where I_0 is the moment of inertia about the axis of the zero spin oscillation. Substituting into (19) the oscillation magnitude from (18) yields the maximum oscillation energy, E_m:

$$E_m = \tfrac{1}{2}(\mu_f g_c / a\omega_n)^2 (I_0 + Ma^2), \tag{20}$$

where μ_f, the maximum value of μ_m, is the dynamic coefficient of friction. The angular frequency of oscillation for the small one degree of freedom rocking motion we have assumed is

$$\omega_n^2 = g_c(\rho - a)/(I_0/M + a^2), \tag{21}$$

where ρ is the local radius of curvature.

If the asymmetry is small ($\xi \approx 0°, 90°$), (20) and (21) may be simplified by realizing that the axes of oscillation will be near the almost coincidental horizontal principal axes of inertia and principal directions of curvature. Thus the principal moments of inertia and principal radii of curvature may be used for I_0 and ρ above to accurately estimate the maximum energy, because these quantities are local minima or maxima; we emphasize that (20) and (21) apply for arbitrary skew, the only approximation being the small motion assumption. Note that for a single body, two maximum energies may be computed, one for each zero-spin oscillatory mode. Presently we are concerned only with the maximum energy, E_{ms}, associated with the *strong* oscillation which, for a zone-I body, will be the dominant oscillation preceding stable spin. The problem now is choosing which principal moment of inertia and radius of curvature pair to use in computing E_{ms}.

At zero spin, the roots of the characteristic equation must be purely imaginary. It can be shown (Bondi 1986) that the roots corresponding to the strong oscillation have the greater magnitude. (A more general definition of the *strong* oscillation, the oscillation of higher frequency at zero spin, is used so that the term may be applied to zone-0 and zone-II rattlebacks as well.) Thus the moment of inertia and radius of curvature which must be used to estimate the maximum energy associated with the strong oscillation are those that maximize (21). Although we assume $\alpha < \beta$, we cannot say in general which of α, β, θ, ϕ the computation will involve (the axis of minimum moment of inertia may be near the direction of maximum or minimum curvature). However, for particular geometric classes of rattlebacks a general statement can be made. For example, for a solid homogeneous elliptic paraboloid (truncated perpendicular to its vertical axis) or a semiellipsoid (truncated along a plane of symmetry)

$$\frac{E_{ms}}{Mga} = \tfrac{1}{2}\mu_{\mathrm{f}}^2 \frac{\alpha^2 \phi}{(1-\phi)}; \quad (E_{ms} = \tfrac{1}{2} M a^2 \gamma n_{ms}^2). \tag{22}$$

In fact this is true for many rattlebacks with a smoothly curved lower surface and a nearly homogeneous mass distribution (including, for example, ellipsoidal shells).

The critical energy for stability derived by Bondi (1986) is a function of the same parameters:

$$\begin{aligned} E_{\mathrm{c1}} &= \tfrac{1}{2}(Mga)\frac{\gamma(1-\theta)(1-\phi)}{(\theta+\phi)+(\alpha+\beta-\gamma)(\theta+\phi-2\theta\phi)-2} \\ &= -\tfrac{1}{2}(Mga)\frac{\gamma(1-\theta)(1-\phi)}{\alpha\beta\theta\phi\mu}. \end{aligned} \tag{23}$$

Although (22) and (23) may be compared, to decide if stable spin may follow a single reversal under the no-slip assumption for any particular set of parameters, this kind of comparison helps us little in understanding the size of the region in the parameter space in which the spin bias can be neatly explained by the possibility of spin-stabilized oscillations. Bondi proposed the θ–ϕ plane for plotting (10), the boundary $\mu = 0$ separating zones 0 and I. The hyperbola $\mu = 0$ depends upon the parameter $(\alpha+\beta-\gamma)$, which is a constant for certain kinds of shapes (even though α, β and γ vary). Hence for a fixed shape we may plot this important boundary and determine the sign of μ based on θ and ϕ alone. In a similar manner, for a homogeneous body of a particular shape, we may write α, β and γ as functions of θ and ϕ and determine the boundary $E_{\mathrm{ms}} = E_{\mathrm{c1}}$. If the shape we assume is symmetric, then the bodies we describe are not rattlebacks, For cases in which the mass distribution is only slightly perturbed, however, the dependence of α, β, and γ on θ and ϕ changes by a small amount. Thus we may determine the subspace of zone I in which stable oscillations may follow a reversal, i.e. the region where $E_{c1} < E_{ms}$. The $\mu = 0$ and $E_{ms} = E_{c1}$ boundaries are plotted for several values of the dynamic coefficient of friction, μ_f, where the assumed shapes are a truncated elliptic paraboloid and a semiellipsoid (figure 5).

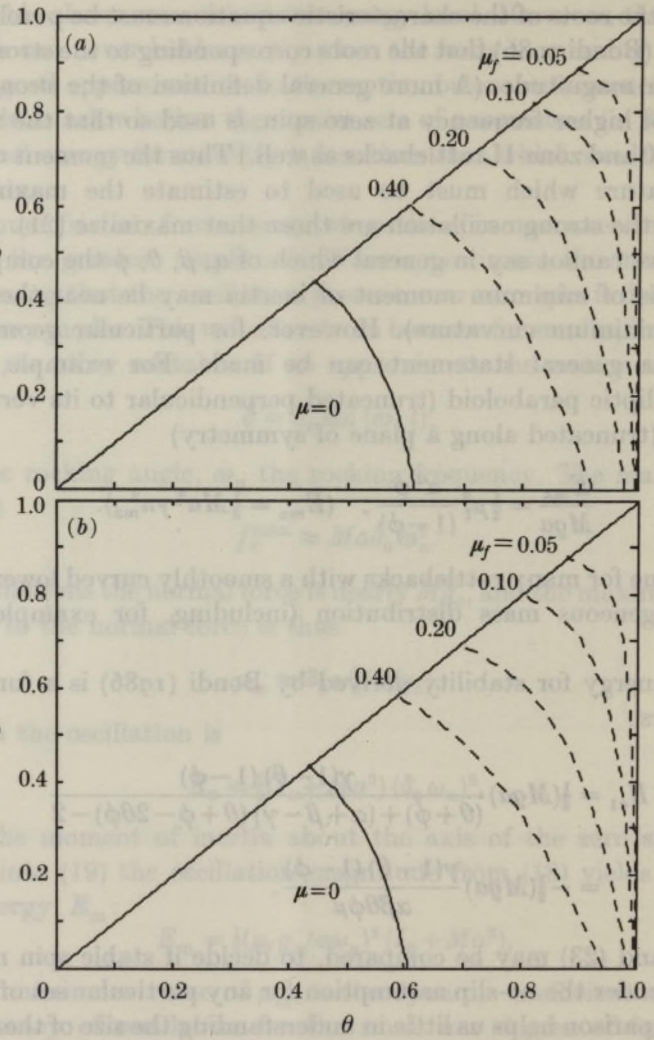

FIGURE 5. Zone-I subspaces in which $E_m > E_{c1}$ for elliptic paraboloid (*a*) and semiellipsoid (*b*) rattlebacks. Regions where asymptotically stable spin is possible after a reversal are to the right of the boundaries labelled with the values of the dynamic coefficients of friction.

Note that all elliptic paraboloid and semiellipsoidal rattlebacks lie in zone 0 or zone I; the curve, $\kappa = 0$, which divides zones I and II is not unique for either shape (as is the hyperbola, $\mu = 0$, dividing zones 0 and I), but it never lies in the region where $\phi < \theta < 1$. Also, the boundaries of zones 0 and I and the curves of $E_{c1} = E_{ms}$ are only slightly different for the two different shapes. Because the critical energy E_{c1} is inversely proportional to μ, it decreases from infinity at the boundary of zones 0 and I to zero at $\theta = 1$. Thus the region where $E_{c1} < E_{ms}$ lies to the right of the curves $E_{c1} = E_{ms}$. The dynamic coefficient of friction between the necessarily hard smooth surfaces of a rattleback and table will usually be less than 0.4. Thus, although all real rattlebacks lying in zone I may spin stably in one direction, only a fraction of these may spin stably after reversing. The latter are characterized by one principal radius of curvature which is only slightly greater than the equilibrium height of the CG.

Many solid rattlebacks with a flat upper surface are close in shape to elliptic paraboloids or semiellipsoids and have only a slight asymmetry. For this important class of bodies (and we suspect for many other shapes) the critical spin velocity, above which both oscillations about equilibrium become stable, is often so large that it is impossible for the body to attain it after reversing spin direction. Yet bodies which exhibit a single reversal are the most common type. Clearly then, the stability of the linearized oscillations of Walker's (1896) no-slip model cannot adequately explain the spin bias exhibited by most rattlebacks. An investigation of the dissipative mechanisms provides a more relevant theory.

4. The dissipative equations

Several mechanisms for creating the non-conservative forces and torques which bring the rattleback to eventual rest come to mind: aerodynamic effects, dry friction due to the contact patch spinning relative to the table, and dry friction due to relative linear motion between the body and the table, and slipping. We now investigate the relative importance of these dissipative effects and determine their role in spin reversals.

(*a*) *The augmented equations of motion*

The air mass exerts dissipative forces and torques on the rattleback as it spins and translates. The complex nature of the rattleback motion makes a precise determination of these effects unnecessarily complicated for the purposes of this study especially because, as is demonstrated in §6, the aerodynamic force and torque are typically at least an order of magnitude smaller than those due to dry friction. The simplest realistic aerodynamic model is a lumped force dependent on the linear velocity and a lumped torque dependent on the angular velocity. For accuracy over the range of Reynolds numbers we shall encounter ($0 < \mathrm{Re} < 10^4$), a quadratic dependence on the velocities is used (White 1979). If we assume that the force acts through the body CG, the aerodynamic force and torque may be approximated by

$$\boldsymbol{f}_{\mathrm{d}} = -\boldsymbol{D}_v[|v_1|v_1 \quad |v_2|v_2 \quad |v_3|v_3]^t, \tag{24}$$

$$\boldsymbol{\tau}_{\mathrm{d}} = -\boldsymbol{D}_\omega[|\omega_1|\omega_1 \quad |\omega_2|\omega_2 \quad |\omega_3|\omega_3]^t. \tag{25}$$

The elements of the matrices $\boldsymbol{D}_v$ and $\boldsymbol{D}_\omega$ are determined from the particular geometry of a rattleback and two-dimensional experimetal flow data (White 1979). Note that with this formulation the aerodynamic force (torque) does not necessarily act in the direction opposite that of the velocity (angular velocity).

As long as the vertical component of the angular velocity is non-zero, a torque referred to as the Coulomb torque also acts on the rattleback. Although point contact is assumed to simplify the kinematics, in reality a small area of the celt contacts the table, and relative angular motion between the surfaces causes this torque. Because we are mainly interested in the average effect of the torque, a useful approximation to its instantaneous value may be

$$\boldsymbol{\tau}_{\mathrm{c}} = -c_{\mathrm{c}}\,\mu_{\mathrm{f}}\,\boldsymbol{u}(Mg)\,\mathrm{sgn}\,(\boldsymbol{u}\cdot\boldsymbol{\omega}), \tag{26}$$

where the approximation is due to the averaging of the normal force and the simplification of the coefficient c_{c}, which must depend dynamically on the contact area, the velocity of the contact area on the body ($\boldsymbol{r}$), the slip velocity ($\boldsymbol{v}_{\mathrm{s}}$), and the magnitude of the spin.

These dissipative terms are added to (1) and (2):

$$M\,\mathrm{d}\boldsymbol{v}/\mathrm{d}t = \boldsymbol{f} - Mg\boldsymbol{u} + \boldsymbol{f}_{\mathrm{d}}, \tag{1$'$}$$

$$\mathrm{d}\boldsymbol{h}/\mathrm{d}t = \boldsymbol{r}\times\boldsymbol{f} + \boldsymbol{\tau}_{\mathrm{d}} + \boldsymbol{\tau}_{\mathrm{c}}. \tag{2$'$}$$

If the contact force, $\boldsymbol{f}$, is eliminated from the equations, no restriction is placed on its magnitude or direction; $\boldsymbol{f}$ takes on whatever value necessary to satisfy the no-slip condition. Realistically, however, the horizontal component of the contact force is limited to some fraction of the normal component. This limiting may be expressed simply by a constant dynamic friction coefficient so that $\boldsymbol{f}$ lies within a cone with apex at the point of contact and half angle equal to μ_{f}. As long as the rattleback rolls without slipping, the contact force varies freely within the cone, but when the body slips, $\boldsymbol{f}$ is constrained to lie on the cone until slipping stops. In fact, when the body spins some slipping must occur whenever the horizontal component of the contact force is non-zero. However, experimental data (§6) indicate that the assumption of no-slip appears to be a valid idealization when the ratio of the tangential reaction force to the normal reaction force is less than the dynamic coefficient of friction.

By further assuming that the slip velocity is in the direction opposite that of the horizontal component of $\boldsymbol{f}$, and that the derivative of the slip velocity has no vertical component, we may determine the slip motion of the rattleback. A new variable, the slip velocity ($\boldsymbol{v}_{\mathrm{s}}$), is introduced. Three additional scalar equations determine the motion:

$$\left.\begin{aligned} |(\boldsymbol{u}\times\boldsymbol{f})\times\boldsymbol{u}| &= \mu_{\mathrm{f}}|\boldsymbol{u}\cdot\boldsymbol{f}|,\\ (\boldsymbol{u}\times\boldsymbol{f})\times\boldsymbol{u}\cdot\boldsymbol{v}_{\mathrm{s}} &= -|(\boldsymbol{u}\times\boldsymbol{f})\times\boldsymbol{u}|\,|\boldsymbol{v}_{\mathrm{s}}|,\\ \mathrm{d}\boldsymbol{v}_{\mathrm{s}}/\mathrm{d}t\cdot\boldsymbol{u} &= 0. \end{aligned}\right\} \tag{27a–c}$$

Equation (6) is modified to

$$\boldsymbol{v} = \boldsymbol{v}_{\mathrm{s}} + \boldsymbol{r}\times\boldsymbol{\omega}. \tag{6$'$}$$

The velocity of the CG is the sum of the non-zero (slip) velocity of the point on the body in contact with the plane surface and the relative velocity of the CG with respect to this intermediate reference point. The contact force now depends on

$\mathrm{d}\boldsymbol{v}_s/\mathrm{d}t$ and to satisfy (27 a, b) we must integrate two components of $\boldsymbol{v}_s$; the third component is determined algebraically because $\boldsymbol{v}_s$ must be perpendicular to $\boldsymbol{u}$. As it turns out, the constraints on f during slipping make it difficult to solve for $\boldsymbol{v}_s$ and $\boldsymbol{\omega}$ explicitly. The state equations may still be solved numerically by using an implicit method. For a discussion of the algorithmic details of handling the transitions from slip to no-slip and vice versa, the reader is referred to Kane & Levinson (1978), although the methods used in that study were slightly different.

These augmented equations are referred to in the sequel as the (complete) numerical model.

(b) *A numerical example*

The substantial differences between solutions of the dissipation-free equations and solutions of the augmented equations developed above are illustrated by simulating (figure 6) with the same geometric and inertial parameters and initial conditions as in the first simulation (figure 2) (additional parameters: $M = 0.25$ kg, $\mu_f = 0.18$, $c_c = 6.23 \times 10^{-4}$ m, $d_{v11} = 4.8 \times 10^{-3}$ kg m^{-1}, $d_{v22} = 1.4 \times 10^{-3}$ kg m^{-1}, $d_{v33} = 1.3 \times 10^{-2}$ kg m^{-1}, $d_{\omega 11} = 5.5 \times 10^{-6}$ kg m^2, $d_{\omega 22} = 1.4 \times 10^{-7}$ kg m^2, $d_{\omega 33} = 2.3 \times 10^{-6}$ kg m^2, all other aerodynamic parameters are zero). Note the realistic spin decay; the maximum spin rate achieved after reversal is much smaller than the initial spin and the spin decays completely after only 9 s. The plot of the ratio of the tangential reaction force to the normal reaction force indicates that slipping has occurred; continuously from about 0.6 to 1.2 s, and then intermittently until about 2.0 s. Notice that when the body slips continuously, the energy rapidly decays to near E_{ms}. The simulation in which the aerodynamic effects and the Coulomb torque are neglected (dashed line) clearly shows that slipping alone can cause this. Because in this particular example $E_{c1} > E_{ms}$, stable oscillations cannot be possible after reversal.

The above example demonstrates the role played by slipping and other dissipation in the behaviour of real rattlebacks. When a body is spun initially in the direction of the strong instability, after it reverses the remaining mechanical energy is at most about E_{ms}. The maximum spin magnitude attainable in the direction of the weak instability is bounded. This fact is readily observed when one experiments with a real rattleback; regardless of how hard it is spun initially, it reverses with a limited spin rate. If enough energy remains so that spin above n_{c1} can be achieved, the body may spin stably for the reason proposed by Bondi (1986). If the critical spin cannot be achieved, whether or not the body reverses again depends on the relative magnitudes of the dissipative torques (aerodynamic and Coulomb) and the reaction torque which causes the reversal (both about the CG).

A numerical model alone is, however, an insufficient tool for understanding the rattleback for two obvious reasons. First, because of their complexity, a precise understanding of how dissipation affects the behaviour is difficult to obtain directly from the dynamic equations. Secondly, despite its complexity, the numerical model is a simplification of a real rattleback. Without any experimental comparisons, the data generated by such a model must be regarded with some doubt. In the remaining part of the paper, a simple model that describes the spin

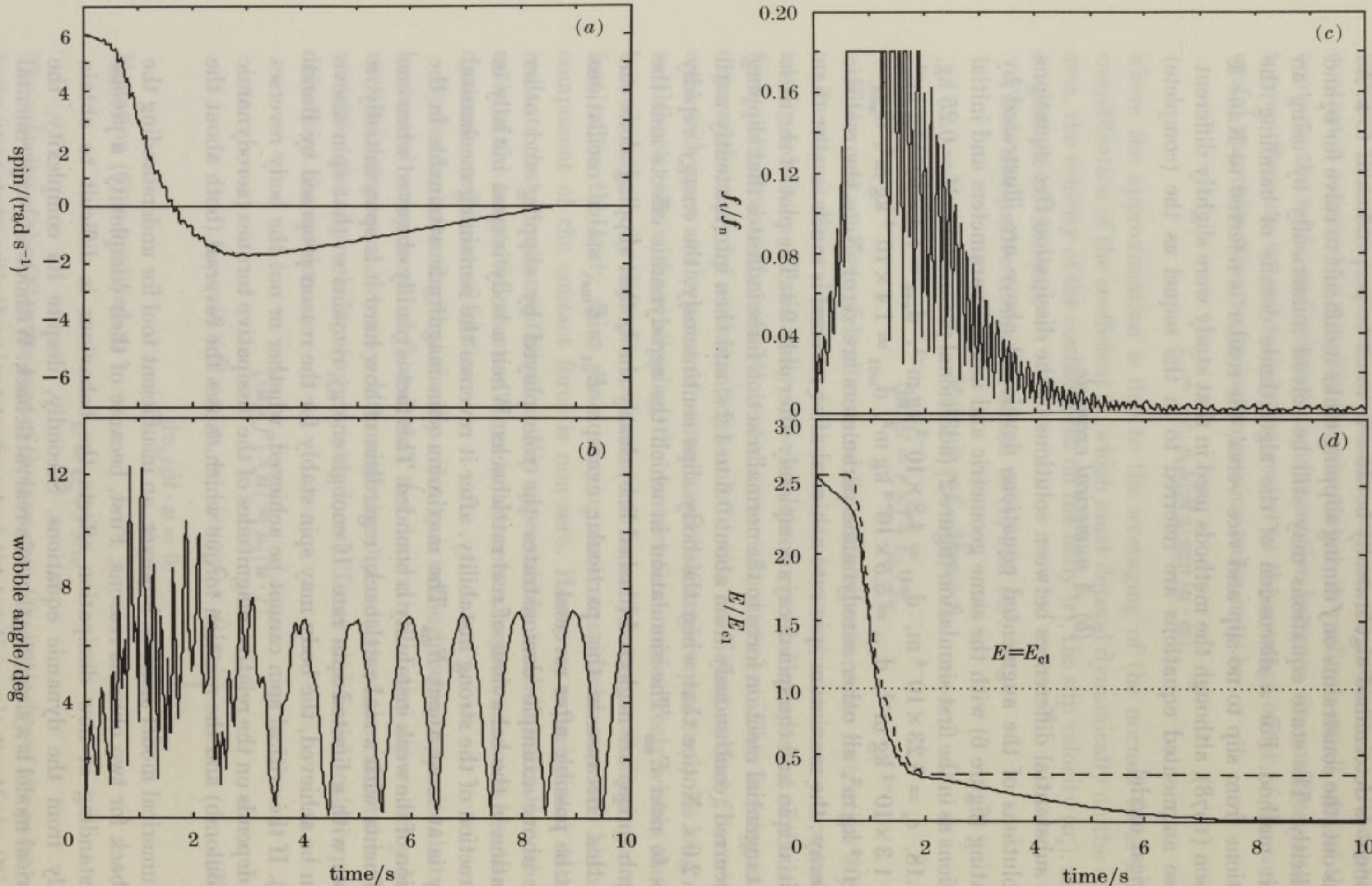

FIGURE 6. Simulated motion of a zone-I rattleback with allowances for dissipation. The solid line of (*d*) indicates the total mechanical energy in the simulation; the broken line is the result from another simulation where the only form of dissipation is sliding; aerodynamic drag and the Coulomb torque are neglected. The initial conditions are the same as those used in the dissipation-free simulation of figure 2.

dynamics is developed by averaging the vertical component of the reaction torque over a period of each modal oscillation. In addition, the numerical simulations are compared with accurate experimental data.

5. Simplified models of the spin dynamics

(*a*) *The mean asymmetric reaction torque*

When dissipation is neglected, the evolution of the spin depends on terms of at least the second degree; these terms provide the coupling between the spin and oscillation energies. These higher-order terms have a significant non-zero mean because, when reversals occur, they dominate dissipative effects which may be of a lower degree (possibly zero for the Coulomb torque). Thus to understand how a reversal takes place, it is important first to understand how these nonlinear terms affect the spin on the average as did Walker (1896) and Breakwell (1974) in their analyses of the evolution of the spin from an oscillatory, zero-spin initial condition.

The exact expression for the inertial vertical component of the reaction torque about the centre of mass, $\boldsymbol{\tau}_v$, when dissipation is neglected is

$$\boldsymbol{\tau}_v = \boldsymbol{u} \cdot \mathrm{d}\boldsymbol{h}/\mathrm{d}t = M\boldsymbol{u} \cdot (\boldsymbol{r} \times \mathrm{d}\boldsymbol{v}/\mathrm{d}t) = M(\boldsymbol{u} \times \boldsymbol{r}) \cdot \mathrm{d}\boldsymbol{v}/\mathrm{d}t. \tag{28}$$

We are interested in computing the average value of $\boldsymbol{\tau}_v$ (28) (hereafter called the *asymmetric torque*) when the motion is a modal oscillation at zero spin.

Integrating by parts we have

$$\frac{1}{M}\int_T \boldsymbol{u} \cdot \mathrm{d}\boldsymbol{h} = \frac{T}{M}\bar{\boldsymbol{\tau}}_v = (\boldsymbol{u} \times \boldsymbol{r}) \cdot \boldsymbol{v}\,|_T - \int_T \boldsymbol{v} \cdot (\boldsymbol{u} \times \mathrm{d}\boldsymbol{r} + \mathrm{d}\boldsymbol{u} \times \boldsymbol{r}). \tag{29}$$

Because the motion is periodic to first order:

$$(\boldsymbol{u} \times \boldsymbol{r}) \cdot \boldsymbol{v}\,|_T = 0. \tag{30}$$

Because $\boldsymbol{v} = \boldsymbol{r} \times \boldsymbol{\omega}$ and, for the linearized motion, $\boldsymbol{r} = \boldsymbol{R}\boldsymbol{u}$:

$$\frac{T}{M}\bar{\boldsymbol{\tau}}_v = -\int_T ((\boldsymbol{R}\boldsymbol{u}) \times \boldsymbol{\omega}) \cdot (\boldsymbol{u} \times (\boldsymbol{R}\mathrm{d}\boldsymbol{u}) + \mathrm{d}\boldsymbol{u} \times (\boldsymbol{R}\boldsymbol{u})), \tag{31}$$

where the elements of $\boldsymbol{R}$ are

$$\left.\begin{aligned} r_{11}/a &= \tfrac{1}{2}[(1+\psi)/\theta + (1-\psi)/\phi]\,\{= -\cos^2\xi/\theta - \sin^2\xi/\phi\},\\ r_{12}/a = r_{21}/a &= -\tfrac{1}{2}(1/\phi - 1/\theta)(1-\psi^2)^{\frac{1}{2}}\,\{= -(1/\phi - 1/\theta)\cos\xi\sin\xi\},\\ r_{22}/a &= -\tfrac{1}{2}[(1-\psi)/\theta + (1+\psi)/\phi]\,\{= -\sin^2\xi/\theta - \cos^2\xi/\phi\},\\ r_{13} = r_{23} &= r_{31} = r_{32} = 0,\\ r_{33}/a &= -1. \end{aligned}\right\} \tag{32a–e}$$

If the integrand is expanded and fourth-order terms are neglected compared with second-order terms, we have

$$\frac{T}{M}\bar{\tau}_v = a\int_T [\omega_1\,\mathrm{d}u_1\,(a+r_{11})+\omega_1\,\mathrm{d}u_2\,r_{12}+\omega_2\,\mathrm{d}u_1\,r_{21}+\omega_2\,\mathrm{d}u_2\,(a+r_{22})], \tag{33}$$

where ω_1, ω_2, $\mathrm{d}u_1$, $\mathrm{d}u_2$ may be obtained from the linearized equations.

If we take $[\omega_1\,\omega_2\,u_1\,u_2]^t$ as the linearized state vector, the system dynamics matrix relating the state vector to its time derivative at zero spin is

$$\boldsymbol{A} = \begin{bmatrix} 0 & 0 & d & e \\ 0 & 0 & f & g \\ 0 & 1 & 0 & 0 \\ -1 & 0 & 0 & 0 \end{bmatrix}, \tag{34}$$

where,

$$d = -g_c\,r_{21}/\alpha a^2, \quad e = -g_c(a+r_{22})/\alpha a^2, \quad f = g_c(a+r_{11})/\beta a^2, \quad g = g_c\,r_{12}/\beta a^2. \tag{35a–d}$$

Notice that d, e, f, g have units of frequency squared and that if the principal axes of inertia and curvature coincide, $d = g = 0$ so that the squares of the frequencies of pitching and rolling would be just e and $-f$. The eigenvalues of $\boldsymbol{A}$ are in general:

$$\lambda_{1,2}^2 = -\tfrac{1}{2}[(e-f)\pm\{[e-f)^2+4(ef-dg)\}^{\frac{1}{2}}]. \tag{36}$$

For convenience we define

$$\lambda_{1,2}^2 = -e', f'. \tag{36$'$}$$

Then the eigenvectors from the $\mathrm{adj}(\lambda\boldsymbol{I}-\boldsymbol{A})$ are the columns of the modal transformation matrix:

$$\boldsymbol{V} = \begin{bmatrix} -e(e'+f)+dg & -e(e'+f)+dg & f'd & f'd \\ -e'g & -e'g & f(f'+e)-dg & f(f'+e)-dg \\ j\surd(e')g & -j\surd(e')g & j\surd(-f')(f'+e) & -j\surd(-f')(f'+e) \\ -j\surd(e')(e'+f) & j\surd(e')(e'+f) & -j\surd(-f')d & j\surd(-f')d \end{bmatrix}. \tag{37}$$

After integrating (33), we find that when the initial conditions are $\frac{1}{2}(\boldsymbol{v}_1+\boldsymbol{v}_2)$ and $\frac{1}{2}(\boldsymbol{v}_3+\boldsymbol{v}_4)$ the average values of the vertical torque are respectively

$$\bar{\tau}_v^e = \tfrac{1}{4}Ma^2\alpha(1/\phi-1/\theta)(1/\alpha-1/\beta)(1-\psi^2)^{\frac{1}{2}}(e')^2\{e(e'+f)-dg\}\,v_e^2,$$

$$\bar{\tau}_v^f = \tfrac{1}{4}Ma^2\beta(1/\phi-1/\theta)(1/\alpha-1/\beta)(1-\psi^2)^{\frac{1}{2}}(f')^2\{f(f'+e)-dg\}\,v_f^2, \tag{38a, b}$$

where the $\boldsymbol{v}_j$ denote columns of $\boldsymbol{V}$ and v_e and v_f are arbitrary scale factors (ω_1, ω_2, u_1, and u_2 are sinusoids readily determined from the eigenvectors and eigenvalues of $\boldsymbol{A}$.)

Clearly, the average torque is zero unless the body is asymmetric ($\psi \neq 1, -1$). Also, the principal radii of curvature and the horizontal principal moments of inertia must be distinct for non-zero $\bar{\tau}_v$. Thus, the same conditions which give rise to the unstable oscillations at non-zero spin and reduce the spin (Bondi 1986) ensure that at zero spin a non-zero mean torque continues to act on the body and causes the completion of reversal. This is not surprising, because the instability of an oscillation at non-zero spin is evidence that the oscillation produces a mean reaction torque which opposes the spin. Hence we have a transfer of energy between the spin and the unstable oscillation. At reversal, when the oscillation has consumed all of the spin energy, and the spin is zero, the torque remains in the same direction and initiates spin opposite the original direction. Now that the torque due to the oscillation and the spin have the same sense, a transfer of energy from the oscillation to the spin occurs and the oscillation becomes stable.

That the mean torques associated with the modal oscillations are necessarily in opposite directions may be demonstrated by proving that the product of τ_v^e and τ_v^f is always negative. Because all other unique factors making up the product are positive, it suffices to show that $\{e(e'+f)-dg\}\{f(f'+e)-dg\}$ is negative:

$$\{e(e'+f)-dg\}\{f(f'+e)-dg\} = \tfrac{1}{2}(ef-dg)\{(e+f)^2-2dg+(e+f)((e+f)^2-4dg)^{\frac{1}{2}}\}. \quad (39)$$

The first factor, $(ef-dg) = -(g/a)^2(1-\phi)(1-\theta)/(\alpha\beta\theta\phi)$, must be negative as $\alpha, \beta, \theta, \phi > 0$, and $\phi < \theta < 1$. The second factor must be positive because the magnitude of $(e+f)^2-2dg$, which is always positive, is always greater than the magnitude of $(e+f)((e+f)-4dg)^{\frac{1}{2}}$, which may be negative if $(e+f) < 0$. Thus, the mean reaction torques associated with the characteristic oscillations are always in opposite directions. The discovery by Walker (1896), and later by Bondi (1986), that the roots of the characteristic equation must be discordant for small enough spin is a manifestation of this fact. Another interesting result easily seen from (38a, b) is the near proportionality, for small enough skew angle ξ, between the asymmetric torque and ξ (because $(1-\psi^2)^{\frac{1}{2}} = 2\cos\xi\sin\xi$).

The mean torque at zero spin for each modal oscillation has been derived to within an arbitrary constant. This arbitrary constant is simply the ratio between the actual magnitude of the modal oscillation and the magnitude of the arbitrarily scaled eigenvectors. A simple manipulation leads to a revealing relation between the mean torque and the oscillation energy. Because each element of V is either purely real or purely imaginary, when a single modal oscillation is present, the contact point always passes through the equilibrium contact point (u_1 and u_3 always become zero simultaneously for this case). At this instant, the mechanical energy of the system is all kinetic and can be written as

$$E_0^e = \tfrac{1}{2}Ma^2[\alpha v_{11}^2+\beta v_{21}^2]\,v_e^2, \quad E_0^f = \tfrac{1}{2}Ma^2[\alpha v_{13}^2+\beta v_{23}^2]\,v_f^2. \quad (40a, b)$$

Thus we find that the total mechanical energy in the oscillations is proportional to the square of the arbitrary scale factors as is the mean torque. Substituting for the scale factors in each of (40a, b) into (38a, b) gives

$$\bar{\tau}_v^f = K^e E_0^e, \quad \bar{\tau}_v^e = K^f E_0^f, \quad (41a, b)$$

$$\left.\begin{aligned} K^e &= \left(\frac{1}{2}\right)\frac{\alpha(1/\phi-1/\theta)(1/\alpha-1/\beta)(1-\psi^2)^{\frac{1}{2}}(e')^2\{e(e'+f)-dg\}}{\alpha(e(e'+f)-dg)^2+\beta(e'g)^2}, \\ K^f &= \left(\frac{1}{2}\right)\frac{\beta(1/\phi-1/\theta)(1/\alpha-1/\beta)(1-\psi^2)^{\frac{1}{2}}(f')^2\{f(f'+e)-dg\}}{\alpha(f'd)^2+\beta(f(f'+e)-dg)^2}. \end{aligned}\right\} \quad (42a, b)$$

The mean reaction torque, at zero spin when a modal oscillation is present, is proportional to the oscillation energy (41). The dimensionless K^e and K^f, defined in (42), are called the *asymmetric torque constants*. Because for no-slip motion the oscillation energy is bounded, the mean reaction torque is bounded also.

The dependence of the asymmetric torque constants on the non-dimensional parameters $(\alpha, \beta, \gamma, \theta, \phi, \psi)$ is complicated; the parameters e, f, d, g, e', and f' are themselves intricately related to the basic parameters. We would like to investigate the variation of the asymmetric torque constants for a large range of asymmetry angles, ξ, when α, β, γ, θ, and ϕ are fixed. As a single demonstrative example, K^e and K^f are plotted in figure 7 with the zone-I example parameter set (§2*c*), except that ξ (and thus ψ) is varied. The behaviour shown is typical of what is observed for a wide range of parameters. The larger (strong) torque constant, associated with the faster (strong) oscillation, varies almost sinusoidally with 2ξ. The peaks at about 45° and 135° where the asymmetry is maximum are what one

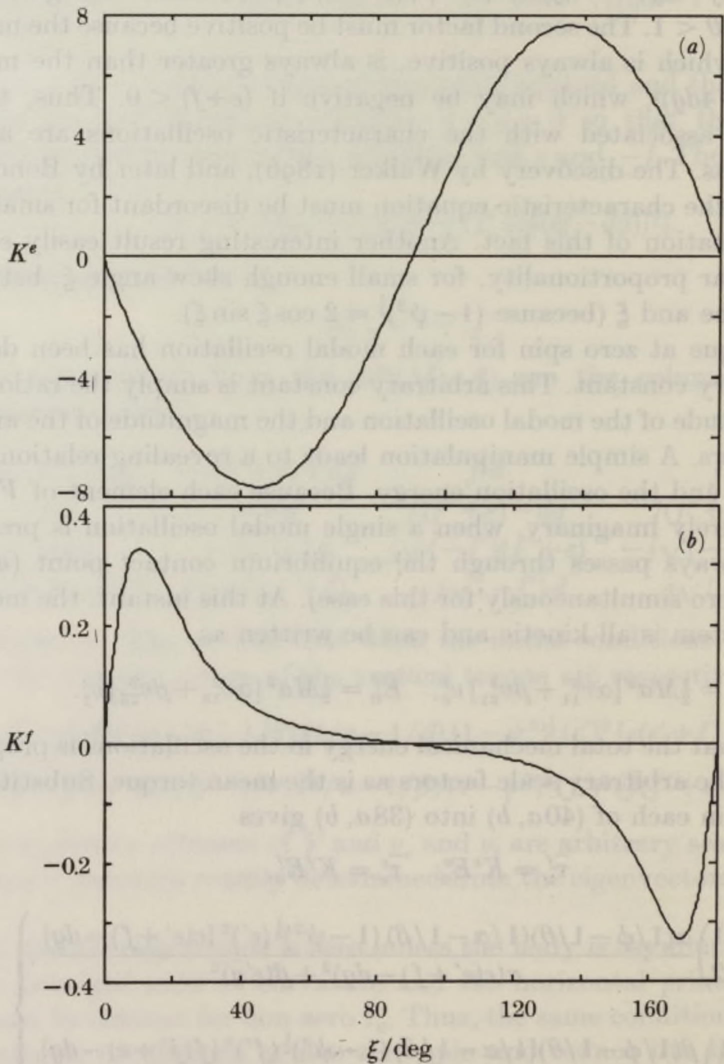

FIGURE 7. Variation in asymmetric torque constants with skew angle.

would expect. The variation in the smaller constant is more surprising. Although nearly proportional to the skew angle for small asymmetry, the peaks do not coincide with maximum asymmetry.

(*b*) *Spin models*

The above study of the vertical reaction torque component during modal oscillations has revealed that the mean asymmetric torque is proportional to the oscillation energy. Strictly speaking this result is valid only at zero spin because the derivation involved integrating the vertical torque over an oscillation period during which the motion was constrained so that the spin was zero. Because the oscillatory modes depend continuously on the spin, (41) may be used to accurately approximate the mean torque in the neighbourhood of zero spin; simulations with the complete model are used presently to demonstrate that the approximation is accurate even for sizeable spin rates. The postulate that the mean asymmetric torque is proportional to the oscillation energy makes possible the derivation of a simple model of the spin behaviour.

Another key observation supporting the development of such an approximate model is the dominance of a single oscillatory mode throughout a single reversal. Note in the simulations (figures 2–5, and 7) that the periods of dominance of the slower and faster frequency are associated with reversal in one or the other direction. Due to the initial condition, both oscillations may be initially present, but the stable oscillation soon diminishes. Such a simplified model will certainly be limited in its range of applicability to some maximum spin because, as Bondi (1986) has clearly shown, the character of the weak oscillation will change significantly (become stable) with large enough spin. It will also be able to deal with only one oscillation at a time.

First we will develop the model for the dissipation-free case. Because energy is conserved, the energy in the single modal oscillation considered is

$$E_0 = \tfrac{1}{2}I_{33}(n_0^2 - n^2), \tag{43}$$

where the initial system energy is expressed as $\tfrac{1}{2}I_{33}\,n_0^2$. The postulate that the torque is proportional to the energy in the oscillation leads to the following spin averaged first-order nonlinear model:

$$\mathrm{d}n/\mathrm{d}t = \tfrac{1}{2}K(n_0^2 - n^2) \tag{44}$$

with general solution

$$n(t) = n_0 \frac{(n_0 + n_i)\exp(Kn_0 t) - (n_0 - n_i)}{(n_0 + n_i)\exp(Kn_0 t) + (n_0 - n_i)}, \tag{45}$$

where n_i is the initial spin. The time to reversal, t_r, defined as the time when $n = 0$, is then

$$t_r = \frac{1}{Kn_0}\ln\left|\frac{n_0 - n_i}{n_0 + n_i}\right|. \tag{46}$$

Equation (46) indicates that the time to reversal is inversely related to the nominal spin n_0 and the parameter K (either K^e or K^f). Also, the time to reversal depends on the fraction of the initial energy in the oscillatory mode: with no energy in the oscillation, no reversal will occur. This relation becomes clearer if we substitute $n_i = -p^{\frac{1}{2}}n_0$ into (46). This gives:

$$t_r = \frac{1}{Kn_0} \ln \left| \frac{(1+p^{\frac{1}{2}})^2}{1-p} \right|, \tag{46'}$$

where the quantity $(1-p)$ is the fraction of the initial energy in the oscillation. If $(1-p)$ is zero, the time to reversal is infinite.

To demonstrate the validity of the simplified model we plot (figure 8*a*) the predicted spin behaviour obtained from a simulation along with the solution of the simplified equation (45). The initial conditions in the simulation are $\boldsymbol{u} = [0\ 0\ -1]^t$, $\omega = [0.6243\ 0.1909\ -2.819]^t$ rad s^{-1}, the parameters in the simplified model are: $K(=K^e) = -0.2766$, $n_0 = -2.892$, and $(1-p) = 0.05$. A more global demonstration of the accuracy of the simple model is the comparison of the analytical time to reversal (plotted continuously and calculated from the simple model (46)) and the simulated time to reversal over the range of nominal spin rates for which slipping will not occur ($\mu_f = 0.18$). In figure 8*b*, the spin is initially in the unsteady direction and $(1-p) = 0.075$; in figure 8*c*, the spin is initially in the steady direction and $(1-p) = 0.25$. Curiously, the simple model overestimates the time to reversal in the unsteady direction and underestimates the time to reversal in the steady direction. The trend toward higher accuracy at smaller nominal spin rates is apparent in both spin directions. The parameter set used in all of these demonstrations is: $\theta = 0.6429$, $\phi = 0.0360$, $\psi = 0.9982$, $\alpha = 13.04$, $\beta = 1.522$, $\gamma = 12.28$, $a = 1.8$ cm ($\mu = -0.2565$, $\kappa = 1.573$, $K^e = -0.2766$, $K^f = 0.04838$, $n_{c1} = 39.91$ s^{-1}, a zone-I body).

As figure 8 shows, the simplified model adequately approximates the spin behaviour of the dissipation-free nonlinear equations. It describes the behaviour for each reversal direction separately and always predicts that a reversal occurs in both directions (unless all of the initial energy is in spin). But this is not what is often observed: many rattlebacks reverse in only one direction. The simple model can be modified to improve its predictive power by including the most important dissipative effects.

First, consider the aerodynamic torque. The linearized aerodynamic model, proposed by Kane & Levinson (1982), is much more convenient to use here than the quadratic model because it leads to a simpler relation between the rate of energy dissipation by aerodynamic effects and the energy in the oscillation.

$$\tau_d = -\sigma\omega. \tag{47}$$

The rate of energy dissipation by this mechanism is:

$$\mathrm{d}E/\mathrm{d}t = -\sigma\omega^{\tau}\omega. \tag{48}$$

This may be divided into two parts, one for the oscillation, and one for the spin:

$$\mathrm{d}E/\mathrm{d}t = -\sigma(\omega_1^2+\omega_2^2)-\sigma\omega_3^2 \approx -\sigma(v_{1j}^2+v_{2j}^2)\tfrac{1}{2}v^2-\sigma n^2, \tag{49}$$

where the factor of one-half in the first term in the last equation comes from averaging over an oscillation. Now, by conservation of energy, the sum of the

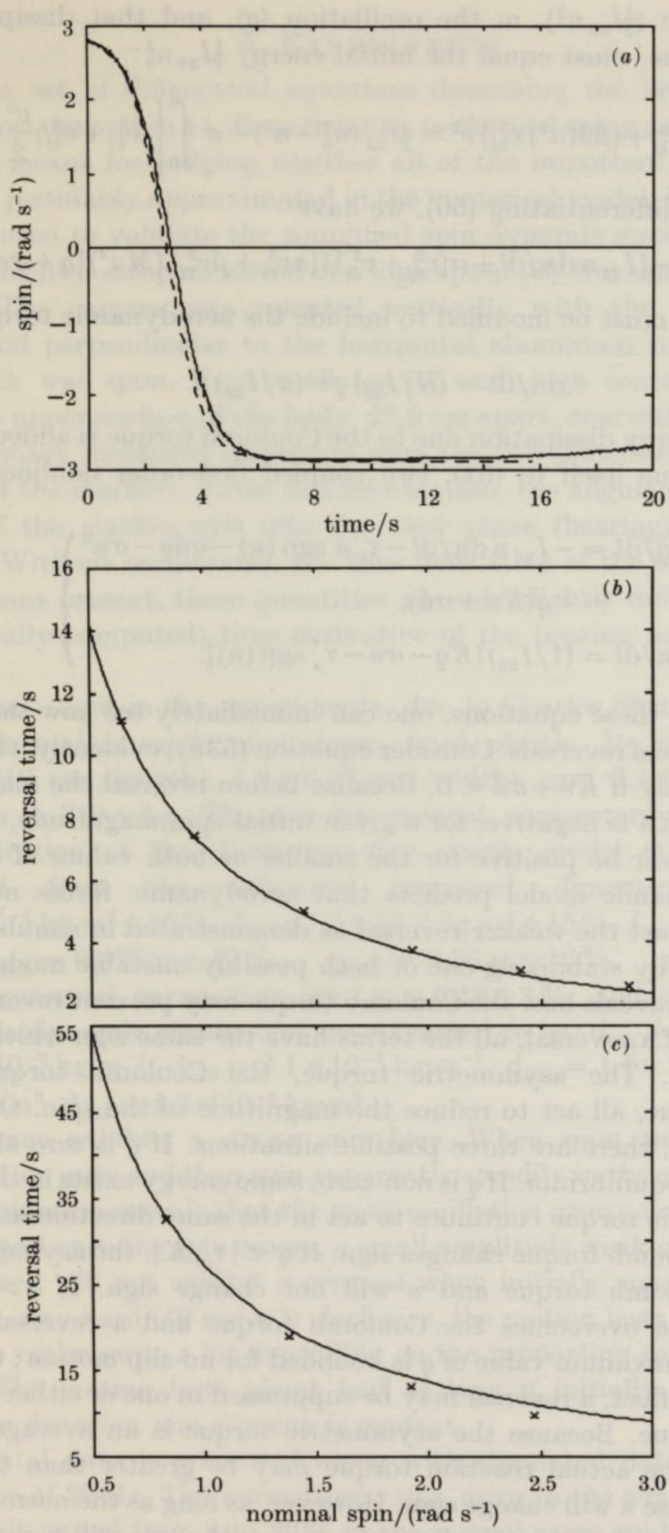

FIGURE 8. Comparison of spin behaviour predicted by the dissipation-free simple models with numerical solutions of the complete dissipation-free equations. (*a*) Spin time histories for strong reversal, $(1-p) = 0.05$. Solid line, complete equations; broken line, simple model. (*b*) Time to reverse against nominal spin. Solid line, simple model; crosses, complete equations. Initially spun in the unsteady direction, $(1-p) = 0.075$, $K = K^e$. (*c*) As (*b*), initially spun in the steady direction, $(1-p) = 0.25$, $K = K^f$.

energy in the spin ($\frac{1}{2}I_{33}n^2$), in the oscillation (q), and that dissipated by the aerodynamic torque, must equal the initial energy $\frac{1}{2}I_{33}n_0^2$:

$$q = \tfrac{1}{2}[(\alpha Ma^2)v_{1j}^2 + (\beta Ma^2)v_{2j}^2]v^2 = \tfrac{1}{2}I_{33}(n_0^2 - n^2) - \sigma \int_0^t \left[(v_{1j}^2 + v_{2j}^2)\frac{v^2}{2} + n^2\right] \mathrm{d}\tau. \quad (50)$$

Rearranging and differentiating (50), we have

$$\mathrm{d}q/\mathrm{d}t = -[I_{33}\, n\, \mathrm{d}n/\mathrm{d}t + \sigma(v_{1j}^2 + v_{2j}^2)\,[(\alpha v_{1j}^2 + \beta v_{2j}^2)\,(Ma^2)]\,q + \sigma n^2]. \quad (51)$$

The spin equation must be modified to include the aerodynamic torque acting on the body:

$$\mathrm{d}n/\mathrm{d}t = (K/I_{33})\,q - (\sigma/I_{33})\,n. \quad (52)$$

If the rate of energy dissipation due to the Coulomb torque is added to (51), and the Coulomb torque itself to (52), two coupled first-order nonlinear equations result:

$$\left.\begin{aligned} \mathrm{d}q/\mathrm{d}t &= -I_{33}\, n\, \mathrm{d}n/\mathrm{d}t - \tau_c\, n\, \mathrm{sgn}\,(n) - \sigma\hat{a}q - \sigma n^2 \\ &= -q(Kn + \sigma\hat{a}), \\ \mathrm{d}n/\mathrm{d}t &= (1/I_{33})\,[Kq - \sigma n - \tau_c\, \mathrm{sgn}\,(n)]. \end{aligned}\right\} \quad (53a, b)$$

Without solving these equations, one can immediately see how the dissipative effects act to suppress reversals. Consider equation (53a); evidently, the oscillation can be unstable only if $Kn + \sigma\hat{a} < 0$. Because before reversal the magnitude of n is decreasing and Kn is negative, for a given initial spin magnitude, it is possible that $\mathrm{d}q/\mathrm{d}t$ can never be positive for the smaller or both values of K. Thus the linearized aerodynamic model predicts that aerodynamic forces may suppress both reversals or just the weaker reversal as demonstrated in simulations (Kane & Levinson 1982) by stabilizing one or both possibly unstable modes.

Equation (53b) reveals how the Coulomb torque may prevent reversals. During the initial phase of a reversal, all the terms have the same sign which is opposite that of the spin. The asymmetric torque, the Coulomb torque, and the aerodynamic torque, all act to reduce the magnitude of the spin. Once the spin diminishes to zero, there are three possible situations. If q is zero also, then the body has reached equilibrium. If q is non-zero, some energy exists in the oscillation and the asymmetric torque continues to act in the same direction as when n was finite, but the Coulomb torque changes sign. If $q < |\tau_c/K|$, the asymmetric torque balances the Coulomb torque and n will not change sign. If $q > |\tau_c/K|$, the asymmetric torque overcomes the Coulomb torque and a reversal occurs. As shown in §3, the maximum value of q is bounded for no-slip motion; thus, as with the aerodynamic effect, a reversal may be suppressed in one or either direction by the Coulomb torque. Because the asymmetric torque is an averaged quantity, instantaneously the actual reaction torque may be greater than the Coulomb torque in which case n will change sign. However, as long as the mean value of the asymmetric torque is less than the Coulomb torque the spin will periodically go to zero and an appreciable spin in the opposite direction will never be achieved.

6. Experiments

A complete set of differential equations describing the behaviour of actual rattlebacks was derived in §4. Experiments, performed using a typical rattleback, are the only means for judging whether all of the important effects have been included and justifiably approximated in the numerical model. Experimental data may also be used to validate the simplified spin dynamic model of §5.

The experimental setup consisted of a high speed (60 Hz) camera and digitizing equipment. The camera was oriented vertically with the viewing direction downward and perpendicular to the horizontal aluminium surface upon which the rattleback was spun. Two small (*ca.* 0.5 cm^2) high contrast markers were affixed to the upper surface of the body, 27.9 cm apart, near either end of the long axis. The primary measured quantities were the two-dimensional coordinates of the centres of the markers. From this information, the angular orientation of the projection of the marker axis into the view plane (bearing) could readily be determined. Without oscillations, the time derivative of the bearing is the spin; with oscillations present, these quantities are only slightly different. We will use the (numerically computed) time derivative of the bearing as a measure of the spin.

The specimen used in the experiments, due to Charles Sherburne, appears to be symmetric and is made of a dense, hard plastic. Its overall dimensions are: 28.7 ± 0.05 cm (length), 4.9 ± 0.05 cm (width), and 3.1 ± 0.05 cm (height), and its mass is 310 ± 2 g. The non-dimensional parameters are those used in the demonstration of the dissipation-free simple model (§5 figure 8); they are derived from the following measured dimensional parameters: $I_{11} = 3.9 \times 10^{-3}\ \mathrm{kg\ m^2} \pm 15\%$, $I_{22} = 1.7 \times 10^{-4}\ \mathrm{kg\ m^2} \pm 15\%$, $I_{33} = 4.0 \times 10^{-3}\ \mathrm{kg\ m^2} \pm 15\%$, $\rho_{\min} = 0.028\ \mathrm{m} \pm 12\%$, $\rho_{\max} = 0.50\ \mathrm{m} \pm 12\%$, $a = 0.018\ \mathrm{m} \pm 6\%$. Additional measured parameters are: $\mu_f = 0.18 \pm 3\%$, and $c_c = 6.1 \times 10^{-4}\ \mathrm{m} \pm 10\%$. The aerodynamic parameters are estimated to be: $d_{v11} = 7.4 \times 10^{-3}\ \mathrm{kg\ m^{-1}}$, $d_{v22} = 1.9 \times 10^{-3}\ \mathrm{kg\ m^{-1}}$, $d_{v33} = 2.1 \times 10^{-2}\ \mathrm{kg\ m^{-1}}$, $d_{\omega 11} = 1.1 \times 10^{-5}\ \mathrm{kg\ m^2}$, $d_{\omega 22} = 1.9 \times 10^{-7}\ \mathrm{kg\ m^2}$, $d_{\omega 33} = 4.3 \times 10^{-6}\ \mathrm{kg\ m^2}$.

The specimen exhibits a strong spin bias. When spun anticlockwise it will reverse direction once and then spin apparently steadily in the clockwise direction. Careful examination reveals that the weak oscillation grows slowly while the spin is clockwise and once the spin ceases, a small amplitude weak oscillation remains. This rattleback will not exhibit a reversal when initially spun clockwise. If the body is spun very hard (40 rad s^{-1}) clockwise, the motion lasts about 40–50 s but the duration varies quite a bit depending on the supporting surface material and roughness. The motion lasts about half as long if initially spun hard in the anticlockwise direction and slipping is evident.

Experimental data is presented along with simulated data in figure 9 at a sampling rate of 30 Hz. The normalized r.m.s. error in the simulation, defined in (54), is 8% (it varied from 8 to 20% in the several cases studied).

$$\epsilon_{\mathrm{r.m.s.}} = \sqrt{\left[\sum_i (n_i^e - n_i^s)^2\right]} \Big/ \sqrt{\left[\sum_i (n_i^e)^2\right]};$$

$$n^e \equiv \text{experimental spin},\ n^s \equiv \text{simulated spin}. \tag{54}$$

Note that in performing the simulation neither the initial condition nor the skew angle, ξ, was precisely known. The data obtained from the two-dimensional video equipment were adequate for estimating the spin but not the general oscillatory state of the rattleback. The initial value of ω_3 was approximated from the initial spin; the rest of the initial state vector was assumed to be a modal oscillation at zero spin for the unstable mode. This is sufficient because the growth of the dominant unstable oscillation depends on its initial magnitude and the total initial energy (§5). We assume that whatever small amount of energy exists in the stable oscillation will not influence the motion significantly. The skew angle was unknown because it is difficult to measure to within the required precision (*ca.* 0.1°).

The unknown oscillation magnitude and skew angle were determined by choosing the values that minimized the error between the experimental and simulated data (54). The skew angle was verified by repeating this procedure several times for data from different experimental trials; it was found to vary by no more than $\pm 6\%$ and the average value of 1.72° was used in the simulation presented here (figure 9). (It is surprising that such a small skew angle can produce such dramatic dynamic behaviour.) The initial oscillation magnitude naturally varied from trial to trial and could not be verified in the same way as the skew angle.

Interestingly, at the low angular velocities necessary to avoid slipping, the aerodynamic influence is very slight. By spinning the rattleback faster (and thus increasing the vertical aerodynamic torque substantially) in the steady direction and comparing experimental data with simulations, the accuracy of the estimated aerodynamic parameters was checked. The dynamic coefficient of friction measured between the experimental specimen and the aluminium surface was $\mu_f = 0.179$. Thus $n_{ms} = 2.876$ rad s^{-1} (22) is a reasonable upper limit on no-slip spin rates. Even at this spin rate, the ratio of the vertical aerodynamic torque to the Coulomb torque is only about 10%. In fact, if the simulation in figure 9 is repeated with $\boldsymbol{D}_\omega = \boldsymbol{D}_v = \boldsymbol{0}$, the results are almost imperceptibly different. It appears as if the aerodynamic influence is small on rattlebacks made of relatively dense materials such as wood or hard plastic.

An alternate simplified model neglecting aerodynamics may be developed in the manner of §5 using the spin, n, and the bearing angle, s (rather than q), as state variables. These state variables are convenient since their values can be determined readily from the experimental data.

$$\frac{\mathrm{d}n}{\mathrm{d}t} = \frac{K}{2}\left(n_0^2 - n^2 - \frac{2\tau_c}{I_{33}}s\right) - \frac{\tau_c}{I_{33}}\operatorname{sgn}(n),$$

$$\mathrm{d}s/\mathrm{d}t = |n|. \qquad (55a, b)$$

Equations (55) are easily solved in the phase plane for periods in which n does not change sign. Complete solutions can be obtained by patching together solutions for the positive and negative spin periods. Taking n to be initially positive, the general solution for n in terms of s is

$$n^2 = n_0^2 - 2(\tau_c/I_{33})s - (n_0^2 - n_i^2)\exp\{-Ks\}. \qquad (56)$$

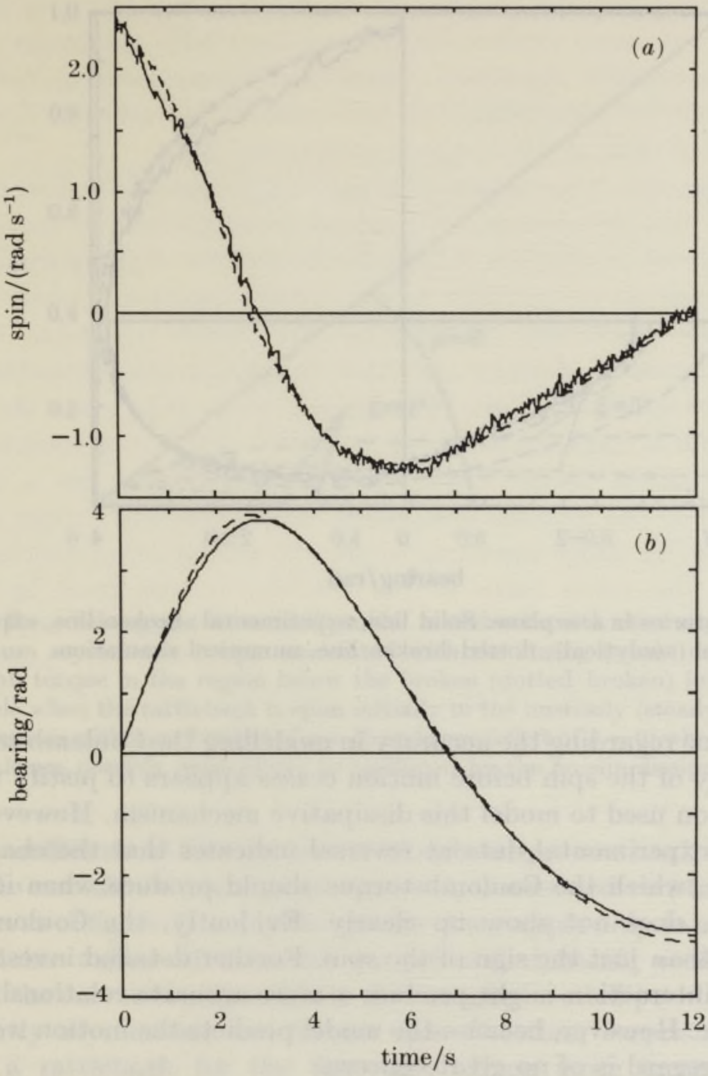

FIGURE 9. Comparison of observed (solid line) and simulated (broken line) behaviour.

For negative n, the only modification required is changing the sign of the second term on the right. The same data that were presented in figure 9 are shown in figure 10 in the phase plane along with the solution to the alternate simplified equations. The match between the experimental data and the data from the complete model is more consistent because the complete equations model both modal oscillations. The alternate simple model predicts the behaviour adequately except near the end of the motion (when the weak oscillation becomes unstable and causes the more rapid spin decay) because the simple model only includes one of the two modal oscillations, in this case the strong one.

Perhaps an oscillation averaged model could be developed which accounted for the spin dependence of the mean asymmetric torque and allowed for both oscillations. Such a model would be extremely tedious, however, to derive, and the additional complexity might make it too unwieldy to yield further insight into the dynamic behaviour.

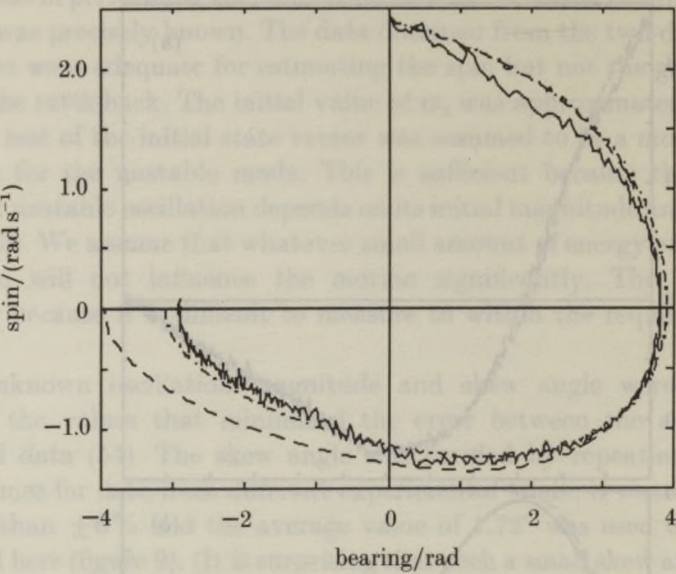

FIGURE 10. Trajectories in s–n plane. Solid line, experimental; broken line, explanatory model (analytical); dotted–broken line, numerical simulation.

A final note is due regarding the accuracy in modelling the Coulomb torque. The nearly linear decay of the spin before motion ceases appears to justify the simple constitutive relation used to model this dissipative mechanism. However, careful inspection of the experimental data at reversal indicates that the characteristic 'kink' in the spin, which the Coulomb torque should produce when it abruptly changes direction, does not show up clearly. Evidently, the Coulomb torque depends on more than just the sign of the spin. Further detailed investigation of the body-surface interaction might produce a more accurate relationship for the dry-friction torque. However, because the model predicts the motion well overall, its failure in this regard is of no great concern.

Although the dissipative torques probably cannot balance the asymmetric torque in as simple a way as indicated in §5, if the maximum asymmetric torque is not greater than the maximum value of the Coulomb damping torque, a significant spin reversal cannot occur. Because the factors contributing to the Coulomb torque are numerous and complicated, its value is best determined by experiment. The maximum value of the asymmetric torque associated with either oscillation may be determined by the theory presented in §3 and §5. (A slight modification is required to determine the maximum energy in the weak oscillation since for large θ, $E_m \to \infty$. For these cases E_m is computed from the potential energy necessary to tip the body over.) To indicate graphically the implications of the present theory we plot (figure 11) the regions in the θ–ϕ plane where one, two or no reversals may occur for roughly semiellipsoidal rattlebacks with different (small) asymmetry angles. The set of rattlebacks for which a spin reversal from the unsteady (steady) direction is likely falls below the broken (dotted–broken) curves; in the semiellipsoidal case, all rattlebacks which reverse from the steady direction also reverse from the unsteady direction. The experimental values of the

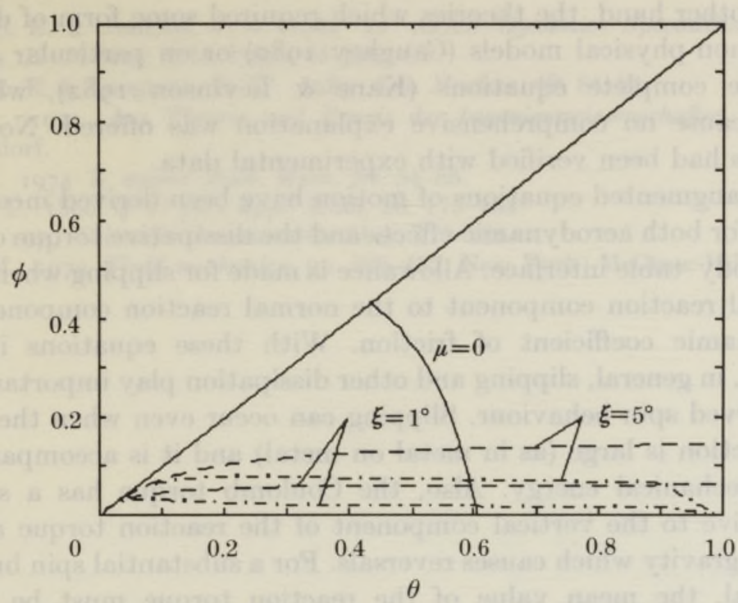

FIGURE 11. Reversal regions for semiellipsoidal rattlebacks with skew angles of 1° and 5°. The maximum asymmetric torque associated with the strong (weak) oscillation exceeds the Coulomb torque in the region below the broken (dotted–broken) line; thus reversals are probable when the rattleback is spun initially in the unsteady (steady) direction. Contrast these regions with zone I (right of $\mu = 0$) and zone 0 (left of $\mu = 0$) where single and multiple reversals are possible respectively as predicted by the no-slip dissipation-free theory.

dynamic coefficient of friction and Coulomb torque are used in determining the curves (the non-dimensional parameter a/c_c is assumed constant).

The curves of figure 11 are quite specific; they apply only to a specific shape and for particular values of Coulomb torque and dynamic coefficient of friction. However, the curves clearly indicate that roughly semiellipsoidal bodies which are only slightly asymmetric can reverse spin direction, surprising to anyone who observes a rattleback for the first time. Even more importantly, figure 11 demonstrates the significant differences between the predictions of Bondi's (1986) no-slip theory and the present theory. Clearly, it is not necessary for a body to lie in zone I for it to exhibit a spin bias; also some zone-I bodies will reverse in both directions.

7. Conclusions

The purpose of this paper has been to explain why real rattlebacks can reverse in one or both directions. Previous successful explanations of the spin bias had neglected all dissipation (including slipping) at one extreme or found some form of it essential at the other. Careful examination of the no-slip dissipation-free theory reveals that unreasonably large values of the friction coefficient are necessary to account for stable spin following a reversal. Also, the dissipation-free model predicts that any rattleback can reverse in either direction if the total mechanical energy is small enough, which is not observed in practice. Further, the degree of asymmetry required for a reversal to be possible cannot be predicted with this theory. On the other hand, the theories which required some form of dissipation were based on non-physical models (Caughey 1980) or on particular numerical solutions of the complete equations (Kane & Levinson 1982), which were unsatisfying because no comprehensive explanation was offered. None of the proposed models had been verified with experimental data.

In this paper augmented equations of motion have been derived incorporating lumped models for both aerodynamic effects and the dissipative torque due to dry friction at the body–table interface. Allowance is made for slipping when the ratio of the tangential reaction component to the normal reaction component would exceed the dynamic coefficient of friction. With these equations it is then determined that, in general, slipping and other dissipation play important roles in commonly observed spin behaviour. Slipping can occur even when the dynamic coefficient of friction is large (as in metal on metal) and it is accompanied by a rapid loss of mechanical energy. Also, the Coulomb torque has a significant magnitude relative to the vertical component of the reaction torque about the body's centre of gravity which causes reversals. For a substantial spin build-up to follow a reversal, the mean value of the reaction torque must be larger in magnitude than the Coulomb torque which acts in the opposite direction. Although particular solutions of the augmented equations can point out the shortcomings of previous theories, the equations themselves are too complicated to provide an insightful picture of the rattleback's behaviour. The simplified spin dynamic model was derived for this purpose.

The basis of the spin model is a relation between the modal oscillation energy and the mean vertical reaction torque. This relation is a simple proportionality at zero spin, but at non-zero spin the assumption of proportionality is still quite accurate; predictions of both the simplified spin model and the complete augmented equations compare favourably with experimental data. The mean reaction torque provides the coupling between the spin and oscillation energies and is a key element, along with slipping and the Coulomb torque, in an understanding of the rattleback's behaviour. The maximum mean reaction torque in each direction depends upon the associated asymmetric torque constant and the maximum oscillation energy which is limited by the onset of slipping. A significant reversal from the unsteady (steady) to the steady (unsteady) spin direction is possible only if the magnitude of the product of the strong (weak) asymmetric torque constant and the maximum energy in the strong (weak) oscillation is greater than the value of the Coulomb torque.

We gratefully acknowledge comments, suggestions and help from L. W. Alaways, A. Y. Arai, A. E. Edelson, J. L. Junkins and P. M. Meier.

References

Bondi, Sir Hermann 1986 *Proc. R. Soc. Lond.* A **405**, 265–274.
Breakwell, J. V. 1974 *Class-Notes Stanford University.*
Caughey, T. K. 1980 *Int. J. Non-linear Mech.* **15**, 293–302.
Kane, T. R. & Levinson, D. A. 1978 *J. appl. Mech.* **45**, 903–909.
Kane, T. R. & Levinson, D. A. 1982 *Int. J. Non-linear Mech.* **17**, 175–186.

Lindberg, R. E. & Junkins, J. L. 1984 In *AIAA Dynamics Specialists Conference, Palm Springs, 17–18 May 1984*. Paper 84-1062-CP.

Lindberg, R. E. & Longman, R. W. 1983 *Acta Mechan.* **49**, 81–94.

Magnus, K. 1971 *Aus Theorie und Praxis der Ingenieurwissenschaften*. Berlin, München, Düsseldorf.

Magnus, K. 1974 *Z. angew Math. Mech.* **54**, 54–55.

Walker, G. T. 1896 *Q. Jl pure appl. Math.* **28**, 175–184.

Walker, J. 1979 *Scientific American* October, 172–184.

White, F. M. 1979 *Fluid mechanics*, pp. 426–437. New York: McGraw-Hill.